Dynamic Organizing Principles of the Plasma Membrane that Regulate Signal Transduction: Commemorating the Fortieth Anniversary of Singer and Nicolson's Fluid-Mosaic Model

Akihiro Kusumi,[1,2] Takahiro K. Fujiwara,[1] Rahul Chadda,[1] Min Xie,[1] Taka A. Tsunoyama,[1,2] Ziya Kalay,[1] Rinshi S. Kasai,[2] and Kenichi G.N. Suzuki[1,3]

[1]Institute for Integrated Cell-Material Sciences (WPI-iCeMS) and [2]Institute for Frontier Medical Sciences, Kyoto University, Kyoto 606-8507, Japan; email: akusumi@frontier.kyoto-u.ac.jp

[3]National Center for Biological Science, Institute for Stem Cell Biology and Regenerative Medicine, Bangalore 560065, India

Annu. Rev. Cell Dev. Biol. 2012. 28:215–50

First published online as a Review in Advance on August 16, 2012

The *Annual Review of Cell and Developmental Biology* is online at cellbio.annualreviews.org

This article's doi: 10.1146/annurev-cellbio-100809-151736

1081-0706/12/1110-0215$20.00

Keywords

single-molecule imaging, mesoscale-domain architecture, molecular diffusion and collision, actin-based membrane skeleton, picket-fence model

Abstract

The recent rapid accumulation of knowledge on the dynamics and structure of the plasma membrane has prompted major modifications of the textbook fluid-mosaic model. However, because the new data have been obtained in a variety of research contexts using various biological paradigms, the impact of the critical conceptual modifications on biomedical research and development has been limited. In this review, we try to synthesize our current biological, chemical, and physical knowledge about the plasma membrane to provide new fundamental organizing principles of this structure that underlie every molecular mechanism that realizes its functions. Special attention is paid to signal transduction function and the dynamic aspect of the organizing principles. We propose that the cooperative action of the hierarchical three-tiered mesoscale (2–300 nm) domains—actin-membrane-skeleton induced compartments (40–300 nm), raft domains (2–20 nm), and dynamic protein complex domains (3–10 nm)—is critical for membrane function and distinguishes the plasma membrane from a classical Singer-Nicolson-type model.

Contents

GENERAL CELLULAR STRATEGIES FOR ORGANIZING THE PLASMA MEMBRANE

Our knowledge of the mechanisms by which the plasma membrane performs its function has been accumulated mostly using biochemical and molecular biological methods. Studies using these methods were powerful in identifying the many molecules and their interactions that are required for membrane functions. However, these results tended to give very static views on how molecules in the plasma membrane generate functions. Meanwhile, many functions of the plasma membrane have been known to depend critically on its dynamic structure (Campelo et al. 2010, Dustin & Depoil 2011, Engelman 2005, Groves & Kuriyan 2010, Lingwood & Simons 2010, Nabi 2011, Platta & Stenmark 2011, Sens et al. 2008, Viola et al. 2010). Recent studies showed that signal transduction, cell migration, and endocytosis and exocytosis of membrane proteins and lipids all depend on the unique restless molecular dynamics and its temporary cessation in the two-dimensional structure of the plasma membrane (Grecco et al. 2011, Harding & Hancock 2008, Kholodenko et al. 2010, Prior & Hancock 2011, Sengupta et al. 2011, Simons & Gerl 2010). These results suggest that, to further advance our knowledge of how the plasma membrane performs its function, we will have to reveal not only which molecules are involved in a particular function but also how these molecules move about, entering and exiting from (being dynamically organized into) dynamic transient substructures of the plasma membrane, i.e., the molecular dynamics and dynamic organizing principles of the plasma membrane. This way, we should be able to clarify fundamental questions such as how particular molecular interactions and reactions occur selectively or faster than others, as well as how a signaling pathway is preferred over others in a certain context.

In recent years, our understanding of the plasma membrane has advanced far beyond the textbook model of Singer & Nicolson (1972). However, these new concepts are only slowly gaining traction outside the field of membrane biophysics. Many colleagues in other areas of biomedical science still consider the plasma membrane as a simple sea of lipids or, worse, as a solid plate, and they describe it as such in major textbooks, reviews, and research papers. Meanwhile, physicists and physical chemists still naively think that the molecular dynamics and interactions in the plasma membrane can be understood by directly applying the knowledge gained by using liposomes and artificially constructed simple membranes.

In this review, we summarize our current knowledge on the molecular dynamics and the organizing principles of the plasma membrane, in simple and concise terms, for biologists, chemists, and physicists who are interested or involved in membrane research. We address the fundamental questions regarding the general rules (the rules of thumb) for organizing the constituent molecules in the plasma membrane.

Many biologists may resist the idea of simple, general rules for biological systems (as opposed to physicists), but they should be reminded of the fact that common architectures and motifs are continuously found for protein structures and functions (Branden & Tooze 1999). Furthermore, consider that virtually all biological membranes on Earth share the common (although peculiar) basic structure of a two-dimensional liquid, consisting of the mosaic-like mixture of lipids and proteins that undergo thermal diffusion in the two-dimensional space (Singer & Nicolson 1972), and that such universality and apparent uniqueness are comparable with those of the double-helical structure of DNA. This strongly suggests the possibility that the fundamental mechanisms for the various functions of the plasma membrane essentially could be

understood by a set of simple principles underlying its dynamic structure, or more specifically, organizing principles of the plasma membrane and the general cellular strategies utilizing them for plasma membrane function. We call these principles and strategies the "membrane mechanisms." Because the lipid bilayer membrane has a thickness of ~4 nm, the three-dimensional nature of the plasma membrane sometimes becomes important for its function. However, for simplicity, within this review we do not deal with such cases. Therefore, we use the term two-dimensional structure throughout.

MEMBRANE MECHANISMS BY HIERARCHICAL THREE-TIERED MESOSCALE-DOMAIN ARCHITECTURE OF THE PLASMA MEMBRANE

As a simple summary of the plasma membrane architecture, we propose a hierarchical organization into three types of mesoscale (2–300 nm) domains (**Figure 1**):

1. Membrane compartment: diameter of 40–300 nm, created via a partitioning of the entire plasma membrane, owing to its interactions with the actin-based membrane skeleton (fence) and transmembrane (TM) proteins anchored to the membrane-skeleton fence (pickets) (**Figures 2–4**). We think this is the most basic and essential domain because it fundamentally distinguishes the plasma membrane from the Singer-Nicolson-type membranes, such as liposomal membranes and other simple artificially reconstituted membranes. Furthermore, the actin-based partitioning of the plasma membrane occurs virtually everywhere in the plasma membrane. Hence, we call the compartments the first tier in the hierarchical architecture of the plasma membrane. Various popular concepts on molecular interactions, movements, and recruitment in the plasma membrane are often incorrect for only one critical reason: They neglect or ignore the membrane compartmentalization by the actin-based membrane skeleton.
2. Raft domain: enriched in cholesterol, glycosphingolipids, and glycosylphosphatidylinositol (GPI)-anchored proteins. It is generally on the scale of 2–20 nm in diameter but could be as large as the entire apical membrane of epithelial cells (Lingwood & Simons 2010). Raft domains are created by various levels of molecular affinities and immiscibilities involving both lipids and proteins, as well as cooperative molecular condensations, within the plasma membrane. Such affinities and condensations are modulated by stimulation-induced dimers and oligomers of raft-associable receptors; thus, these domains are important for signal transduction and molecular trafficking. We call the raft domain the second-tier domain in the hierarchy.
3. Dynamic protein complex domains: dimers/oligomers and greater complexes of membrane-associated and integral membrane proteins, with sizes generally between 3 nm and 10 nm in diameter (this can extend to a few hundred nanometers, as in the cases of clathrin-coated pits). These protein-based molecular complexes constitute the third-tier mesodomain in the hierarchical architecture. The difference between the second-tier raft domain and the third-tier dynamic protein complex domain is not in the size or number of involved molecules per domain, but rather in the basic interactions that form the domain: Lipid interactions play critical roles for raft-domain formation. As we discuss below, the raft domain may consist of only a few molecules; therefore, the difference between the terms domain and molecular complex becomes meaningless. For the sake of consistency, we refer to both of these molecular assemblies as domains. Meanwhile, because protein-protein interactions are one of

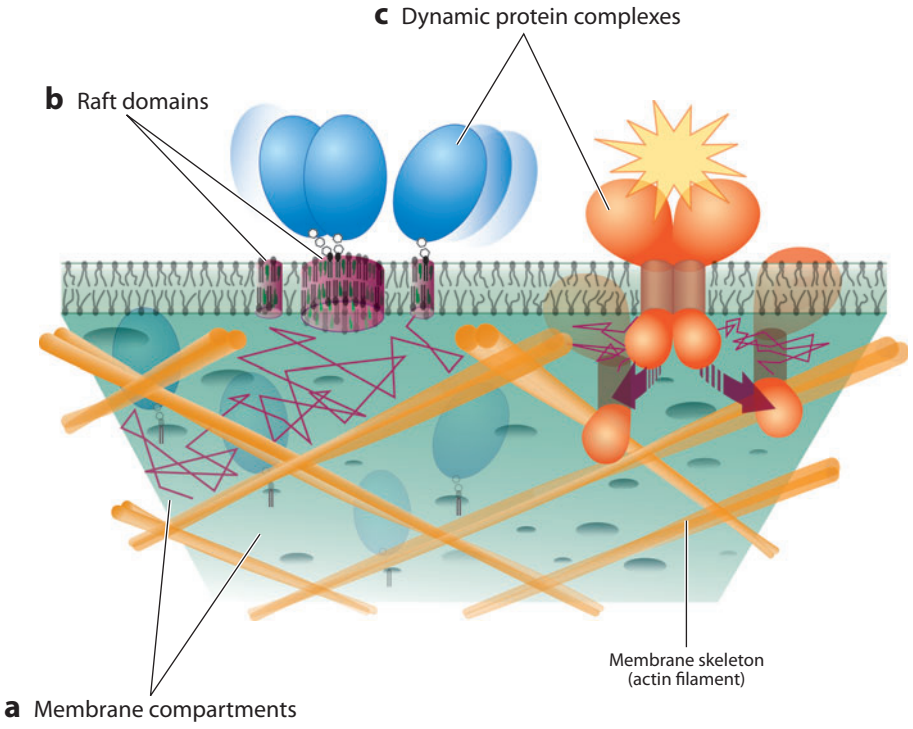

Figure 1

Three-tiered hierarchical mesoscale-domain architecture of the plasma membrane. (*a*) Membrane compartments, generated by the partitioning of the entire plasma membrane by the membrane-associated actin-based membrane skeleton (fence) and transmembrane (TM) proteins anchored to the membrane-skeleton fence (pickets, not shown in this figure). (*b*) Raft domains enriched in cholesterol, glycosphingolipids, and glycosylphosphatidylinositol (GPI)-anchored proteins, with sizes limited by the membrane compartments. (*c*) Dynamic protein complex domain composed of dimers and greater oligomers of integral membrane proteins, which may exist only transiently. This type of domain also includes coat-protein-induced and scaffolding-protein-induced protein assemblies.

the major driving forces in the formation of many raft domains, we consider the raft domains as the second tier and the protein complex domains as the third tier. In this review, such dynamic protein complexes include not only those within the plasma membrane (i.e., those composed of integral membrane proteins), but also those induced by cytoplasmic scaffolding proteins and coat proteins (Bauer & Pelkmans 2006, Doherty & McMahon 2008, Kirchhausen 2009, McMahon & Boucrot 2011, Mercer et al. 2010, Suetsugu et al. 2010, Wilbur et al. 2005).

In this review, we hope to provide convincing evidence that this hierarchical three-domain organization of the plasma membrane is not only reasonable, but also useful, because it provides a clear dynamic and structural perspective for understanding the working mechanisms of the plasma membrane. On the basis of the literature and our own recent single-molecule imaging studies, we explain how these different domains form and how domains at different levels in the hierarchy exclude and interact with each other to generate membrane functions. Recent developments in single-molecule techniques that are applicable to the studies of living cells have provided

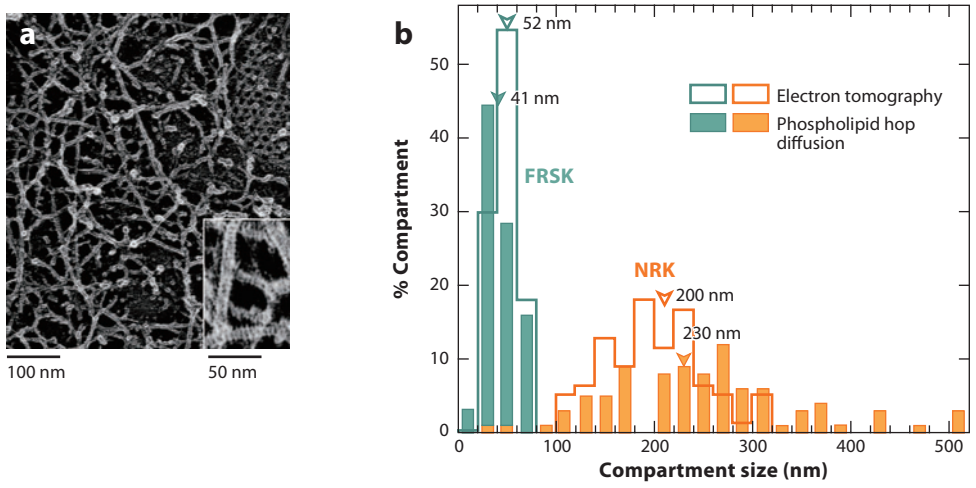

Figure 2

(*a*) Electron microscopic image of the membrane skeleton (MSK) attached to the cytoplasmic surface of a fetal rat skin ketatinocyte (FRSK) cell. The inset highlights the 5.5-nm periodic striped pattern in each individual filament, showing that the membrane skeleton is primarily composed of actin filaments. (*b*) Comparison of the distributions of the MSK mesh size on the cytoplasmic surface of the plasma membrane estimated by electron tomography (*open bars*) with that of the compartment size determined from the phospholipid diffusion data (*closed bars*) for normal rat kidney (NRK, *orange*) and FRSK (*green*) cell lines. Within the same cell type, the MSK mesh size and the diffusion compartment size exhibited similar distributions (compare the open and closed bars with the same color). The actual sizes are quite different between NRK and FRSK cells.

researchers the unprecedented ability to observe directly the movement, assembly, and activation of individual molecules in the plasma membrane (Dustin & Depoil 2011, Kusumi et al. 2005, Murakoshi et al. 2004, Saxton & Jacobson 1997, Toomre & Bewersdorf 2010). These results have set the stage for the discovery of membrane mechanisms. Therefore, our discussion in this review primarily relies on the results obtained by these newer techniques.

We place special emphasis on the actin-based membrane-skeleton-induced compartments, because they make the plasma membrane entirely different from the Singer-Nicolson membrane and artificial membranes, except for those including the partitioning effect (Chang et al. 1981, Mossman et al. 2005, Takimoto et al. 2009). Furthermore, the interaction of the actin-based membrane skeleton with the second- and third-tier mesoscale domains, i.e., raft domains and dynamic protein complex domains, plays key roles in a variety of plasma membrane functions. Owing to space limitations, we avoid comprehensively reviewing raft domains and dynamic protein complexes but instead concentrate on their relationships with the actin-induced compartments. A more comprehensive review on these two mesodomains, which will be complementary to the present review, has been published elsewhere (Kusumi et al. 2012).

WHY MESOSCALE DOMAINS?

The mesoscale represents roughly 2–300 nm, i.e., greater than a nanometer and smaller than a micron. We employ the mesoscale concept because both thermal fluctuations and weak cooperativity in molecular interactions could play important roles. Their combinations appear to be critical mechanisms for various functions and molecular events in the plasma membrane. We try to avoid the term nanoscale, because it gives the impression of static structures and

lack of cooperativity, owing to the small numbers of involved molecules. We hope to convey the idea of dynamic, restless, and cooperative domains and molecular complexes, which continually form and disperse in/on the plasma membrane on various timescales. Furthermore, it would be misleading to refer to a domain with a 300-nm diameter as a nanodomain, because it is 300-fold larger than 1 nm.

THE IMPACT OF A FACTOR OF 20: SLOWER DIFFUSION IN THE PLASMA MEMBRANE AS COMPARED WITH ARTIFICIAL MEMBRANES

For over 30 years, researchers interested in molecular dynamics, signal transduction, or the many functions of the plasma membrane have been confronted by an enigma. However, the real issue was that the problem, or often the logical contradiction, was generally unrecognized as an enigma. This enigma is shown in **Tables 1** and **2** for lipids and TM proteins, respectively. The diffusion coefficients for both proteins and lipids in the plasma membrane are smaller than those found in artificially reconstituted membranes and liposomal membranes, by factors of 5 to 50; a factor of 20 is a good round number to keep in mind. Note that here the diffusion coefficients are those measured on length scales greater than 300 nm, using methods such as fluorescence recovery after photobleaching or fluorescence correlation spectroscopy, or those observed by single-fluorescent-molecule tracking or single-particle tracking at the normal video rate (time window of approximately 100 ms) or at slower rates. In this review, we call these macroscopic diffusion coefficients.

A 20-fold decrease in the macroscopic diffusion coefficient should be difficult to miss. However, for more than 30 years, it has been missed and neglected in most experimental and theoretical studies regarding the dynamic structure of the plasma membrane. In theoretical studies, the predictions were usually not compared directly with the absolute values of the diffusion coefficients obtained experimentally,

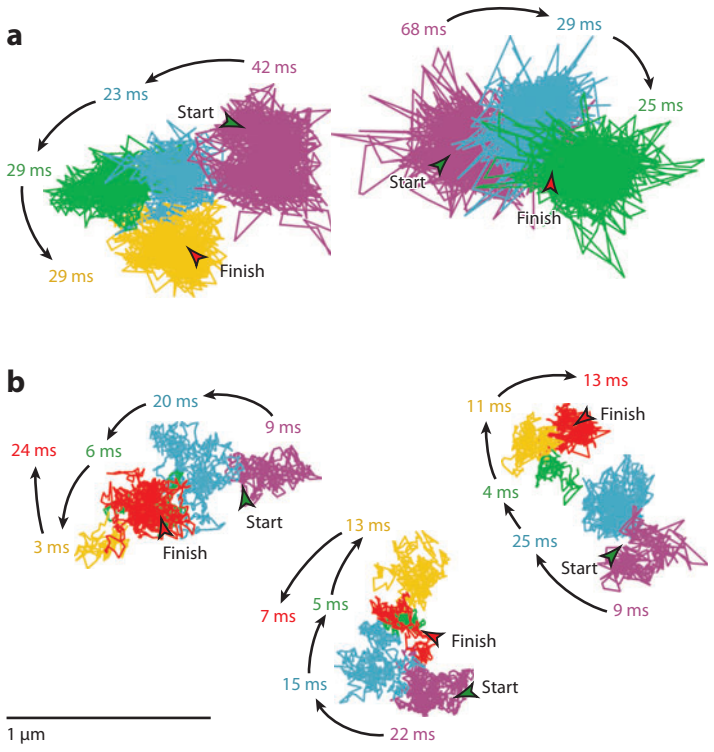

Figure 3

Typical single-molecule trajectories of (*a*) μ-opioid receptor [a G-protein-coupled receptor (GPCR)] and (*b*) an unsaturated phospholipid, using colloidal gold particles as a probe and recorded at a time resolution of 25 μs in the living-cell plasma membrane. Each trajectory was color coded after performing a quantitative analysis that detects jumps between adjacent compartments (developed in our laboratory; applied only to the trajectories classified into the confined-hop diffusion mode). The residency time in each compartment is indicated.

mostly owing to their inclusion of fit parameters and/or the unknown two-dimensional viscosity. No comparisons have ever been made between the diffusion coefficients obtained in both artificial and plasma membranes in theoretical studies. Quite often, only the "relative" changes in the diffusion coefficients, with variations of temperature and/or diffusant sizes, were compared with those obtained experimentally (for example, see Gambin et al. 2006). However, the accuracies of the experimental data are often insufficient for a comparison of the relative changes (and/or the theoretical predictions based on very different models and theories often provided similar dependencies in practical

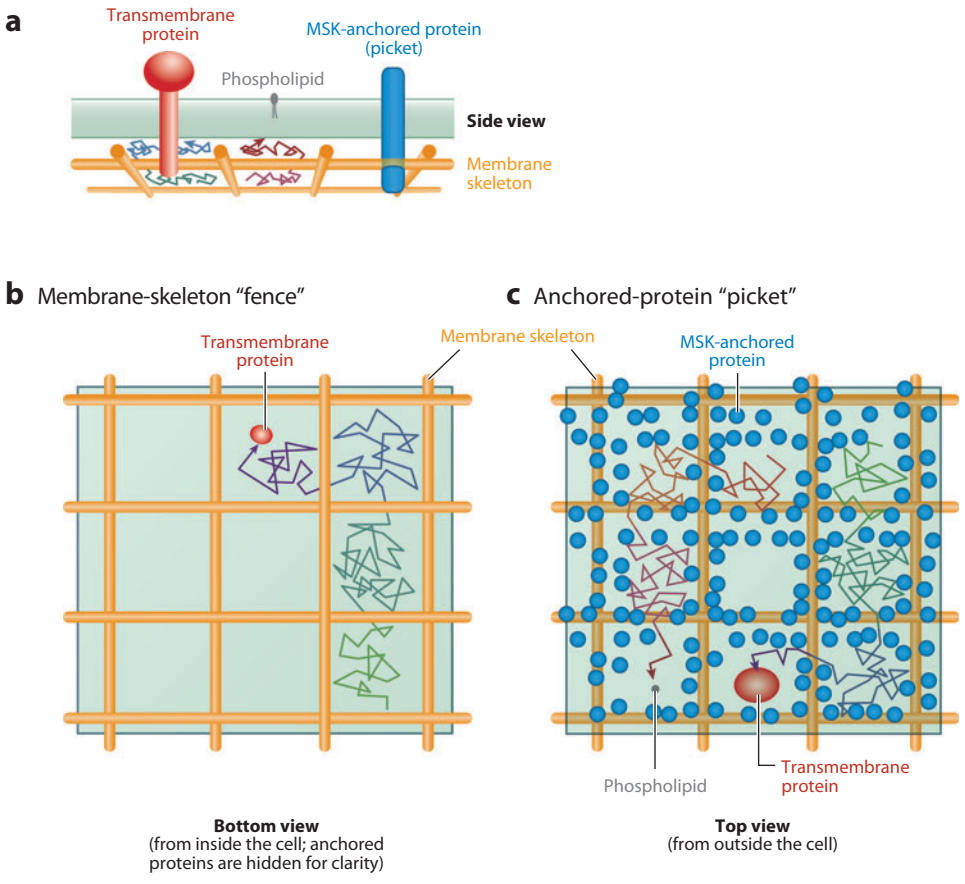

terms), although, in many cases, the theoretical predictions are apparently better with comparisons made with the data on artificial membranes (Liu et al. 1997, Peters & Cherry 1982, Vaz et al. 1982).

In a similar way, this 20-fold difference has also been largely neglected in experimental studies. Biological researchers often paid more attention to the relative changes in the diffusion coefficient they observed, e.g., those of the receptor upon stimulation. As a result, they tended to use theories that were often developed for molecules in artificial membranes to interpret the relative changes they observed; thus, they frequently reached the wrong conclusions.

THE ACTIN-BASED MEMBRANE SKELETON IS RESPONSIBLE FOR SLOWING DIFFUSION BY A FACTOR OF 20

Experimental results in which macroscopic diffusion was examined in both artificial and plasma membranes are rare. However, these analyses could be done more readily, and with more relevance to cell biology, by preparing the blebbed plasma membrane in which the actin cytoskeleton is removed from the cytoplasmic surface of the plasma membrane. The blebbed membrane is a balloon-like protrusion of the plasma membrane, which could also be detached from the rest of the plasma membrane; further removal of actin filaments using drugs such as latrunculin and cytochalasin can also be accomplished (Baumgart et al. 2007; Fujiwara et al. 2002; Kaiser et al. 2009; Levental et al. 2010, 2011).

Fujiwara et al. (2002) showed that, by removing the actin-membrane skeleton (i.e., by using plasma membrane blebs), the macroscopic diffusion coefficient of phospholipids increased by a factor of ~20 (to ~8 $\mu m^2\ s^{-1}$) from that of the intact plasma membrane. This value is comparable to those observed in artificial liposomal membranes. Such plasma membrane blebs are frequently used in raft domain studies to observe the micronscale-domain formation in the plasma membrane at lower temperatures (~10°C) (Baumgart et al. 2007, Kaiser et al. 2009, Lingwood et al. 2008). Such large increases in the macroscopic diffusion coefficient after actin removal were found for TM proteins (T.K. Fujiwara & A. Kusumi, unpublished observations) as well as GPI-anchored proteins (R. Chadda & A. Kusumi, unpublished observations).

These results clearly show that the 20-fold decrease in the diffusion coefficient in the plasma membrane, as compared with that in the simple Singer-Nicolson-type membrane (such as artificial reconstituted membranes, liposomal membranes, and the blebbed plasma membranes), is due to the influence of the actin filaments on the cytoplasmic surface of the plasma membrane. The data also clearly

Figure 4

(*a*) Schematic side view of the plasma membrane, showing the membrane skeleton (MSK), the diffusing transmembrane (TM) protein (*red*), and a TM protein anchored to the MSK, acting as a picket (*blue*). (*b*) The membrane-skeleton "fence" model (the bottom view of the plasma membrane, i.e., the view from inside the cell) and (*c*) the anchored TM protein "picket" model (the top view of the plasma membrane, i.e., the view from outside the cell). The plasma membrane may be partitioned into closely apposed domains (compartments) for the translational diffusion of membrane molecules. All the membrane-constituent molecules undergo short-term confined diffusion within a compartment and long-term hop movement between compartments (hop diffusion). The compartment boundaries are composed of the actin-based MSK (fence) and the TM proteins anchored to and aligned along the actin fences (pickets, including the TM proteins transiently bound to the actin fences). (*d*) The diffusion of molecules in the region around the immobilized TM proteins (*reddish-orange region*) is slower, owing to the hydrodynamic-friction-like effect at the surface of the immobilized protein. This effect could propagate over distances equivalent to multiple diameters of picket proteins. When such diffusion barriers are aligned along the membrane-skeleton fence, they form effective compartment boundaries.

Table 1 Diffusion coefficients (D) for lipids in artificial and cell membranes

Probe[a]	Membrane type[b]	Method[c]	Mobile fraction (%)	D mean (±SD) ($\mu m^2\ s^{-1}$)	Time window for D (ms)	Temperature (°C)	References
Artificial membranes							
Cy5-DPPE	POPE:POPC = 7:3 (free-standing)	SFD	100[f]	20.6 (±0.9)	40	23	Sonnleitner et al. (1999)
EYPC	100% EYPC (multilamellar liposome)	NMR	NA	5 (±2)	~100	35	Lindblom et al. (1981)
NBD-DPPE	100% POPC (free-standing)	FRAP	98	13 (±1.2)	500[j]	23	Ladha et al. (1996)
NBD-PE[d]	100% DMPC (SPB on glass)	FRAP	~100	7.6 (±0.3)	2,000[j]	30	Chang et al. (1981)
NBD-PE[d]	erythrocyte total lipid (SPB on glass)	FRAP	~100	3.4 (±0.3)	4,000[j]	30	Chang et al. (1981)
NBD-eggPE	100% DMPC (coplanar multibilayer)	FRAPP	NA	5 (±0.3)	~3,000[k]	26	Smith et al. (1980)
NBD-DMPE	100% DMPC (multilamellar liposome)	FRAPP	NA	4.3 (±0.2)	~3,000[k]	32	Smith et al. (1980)
Gold-DOPE	eggPC:PS: DOPE = 500:50:1 (GUV)	SPT	100	9.4 (±3.7)	100	37	Fujiwara et al. (2002)
FITC-DPPE	DOPC:DOPE: SAINT-2 = 10:3:1.3 (GUV)	FCS	100[f]	20	~1[l]	RT	Kahya et al. (2001)
NBD-PC[e]	100% DLPC (SPB on mica)	FRAP	100[f]	8.5	~500[j]	25	Ratto & Longo (2002)
Rhodamine Red-X DPPE	100% DOPC (SPB on mica)	FCS Z-scan	100[f]	4.2 (±0.4)	4-35[l]	23	Benda et al. (2003)
NBD-OPPC	100% POPC (SPB on glass)	FRAP	100[f]	8.0 (±2.2)	NA	25	Febo-Ayala et al. (2006)
BODIPY-DPPE	PE:PS:PC[d] = 5:3:2 (free-standing)	SFMT	NA	4.81 (±2.05)	NA	RT	Ichikawa et al. (2006)
DPPE-OG	100% POPC (SPB on quartz)	FCS	100[f]	9.9 (±0.6)	~2[l]	RT	Samiee et al. (2006)
TR-DPPE	DPPC: cholesterol = 8:2 (GUV)	SFMT	100[f]	2.2	33	RT	Ciobanasu et al. (2010)

Cellular plasma membranes							
Cy5-DMPE	HASM	SFD	100	0.6 (±0.04)	12	RT	Schütz et al. (2000)
Cy3-DOPE	NRK	SFMT	100[g]	0.41 (±0.13)[h]	100	37	Fujiwara et al. (2002)
Cy3-DOPE	CHO-B1	SFMT	100[g]	0.30 (±0.23)[h]	100	37	Murase et al. (2004)
Cy3-DOPE	ECV304	SFMT	100[g]	0.22 (±0.14)[h]	100	37	Murase et al. (2004)
Cy3-DOPE	FRSK	SFMT	100[g]	0.27 (±0.20)[h]	100	37	Murase et al. (2004)
Cy3-DOPE	HEK293	SFMT	100[g]	0.41 (±0.18)[h]	100	37	Murase et al. (2004)
Cy3-DOPE	HEPA-OVA	SFMT	100[g]	0.37 (±0.43)[h]	100	37	Murase et al. (2004)
Cy3-DOPE	HeLa	SFMT	100[g]	0.31 (±0.31)[h]	100	37	Murase et al. (2004)
Cy3-DOPE	Melanocytes	SFMT	100[g]	0.40 (±0.28)[h]	100	37	Murase et al. (2004)
Cy3-DOPE	PtK2	SFMT	100[g]	0.53 (±0.30)[h]	100	37	Murase et al. (2004)
NBD-PC[d]	3T3-B	FRAP	54	0.19 (±0.11)	~10,000[j]	NA	Swaisgood and Schindler (1989)
NBD-PC[d]	KMSV-3T3	FRAP	70	0.35 (±0.23)	~10,000[j]	NA	Swaisgood and Schindler (1989)
FITC-DPPE	C3H (lamella)	FRAP	69	0.54 (±0.27)	~350–700[m]	RT	Lee et al. (1993)
FITC-DPPE	PtK1 (lamella)	FRAP	71	0.63 (±0.13)	~350–700[m]	RT	Lee et al. (1993)
FITC-DPPE	Fish-scale fibroblast	FRAP	74	0.95 (±0.17)	~350–700[m]	RT	Lee et al. (1993)
TRITC-DPPE	CHO	SFMT	NA	~0.2 [80%] ~2 [20%]	30.8	22	Nishimura et al. (2006)
BODIPY FL-C_5-PC	COS-7	FCS	100[f]	~1.3	12-24[l]	37	Lenne et al. (2006)
BODIPY FL-C_5-PE	COS-7	FCS	100[f]	~1.4	NA	37	Lenne et al. (2006)
BODIPY FL-C_5-PC	COS-7	FCS in nanoaperture	100[f]	0.95 (±0.10)	7-13[l]	27	Wenger et al. (2007)
QD-DHPTE	COS-7	SPT	NA	1.07	100	NA	Murcia et al. (2008)
QD-DHPTE	HEK293	SPT	NA	0.70	100	NA	Murcia et al. (2008)
QD-DHPTE	COS-7	SPT	NA	0.63		NA	Murcia et al. (2008)
Alexa594-DOPE	CHO	SFMT	100	0.15 (±0.015)[i]	100	37	Umemura et al. (2008)
Atto647N-PE	PtK2	STED-FCS	100[f]	0.5 (±0.2)	0.5-20[l]	27	Eggeling et al. (2009)
Atto647N-PE	PtK2	Confocalized single-molecule tracking	70	0.4	10	23	Sahl et al. (2010)

(*Continued*)

Table 1 (*Continued*)

Probe[a]	Membrane type[b]	Method[c]	Mobile fraction (%)	D mean (±SD) ($\mu m^2\ s^{-1}$)	Time window for D (ms)	Temperature (°C)	References
Atto647-DOPE	Boar sperm: equatorial segment	SFMT	61	0.36 (±0.04)[i]	225	23	Bruckbauer et al. (2010)
Atto647N-PE	PtK2	STED-FCS	100[f]	~0.5	0.5-20[l]	25	Mueller et al. (2011)
Atto647N-PE	HeLa	STED-FCS	100[f]	~0.3	NA	25	Mueller et al. (2011)
Atto647N-PE	CHO	Confocal and NSOM-FCS	100[f]	0.49	1.2-23[l]	25	Manzo et al. (2011)

[a]BODIPY-DPPE, *N*-(BODIPY 530/550)-1,2-dipalmitoyl-*sn*-glycero-3-phosphoethanolamine; BODIPY FL-C_5-PC, 2-(4,4-difluoro-5,7-dimethyl-4-bora-3a,4a-diaza-s-indacene-3-pentanoyl)-1-hexadecanoyl-*sn*-glycero-3-phosphocholine; BODIPY FL-C_5-PE, 2-(4,4-difluoro-5,7-dimethyl-4-bora-3a,4a-diaza-s-indacene-3-pentanoyl)-1-hexadecanoyl-*sn*-glycero-3-phosphoethanolamine; DMPE, 1,2-dimyristoyl-*sn*-glycero-3-phosphoethanolamine; DOPE, 1,2-dioleoyl-*sn*-glycero-3-phosphoethanolamine; DPPE, 1,2-dipalmitoyl-*sn*-glycero-3-phosphoethanolamine; DPPE-OG, *N*-(Oregon Green 488)-1,2-dipalmitoyl-*sn*-glycero-3-phosphoethanolamine; ECV304, human epithelial cells (the same as T24); EYPC, egg-yolk phosphatidylcholine; FITC, *N*-(fluorescein isothiocyanate); FRSK, fetal rat skin keratinocyte; HEK293, human embryonic kidney; HEPA-OVA, mouse hepatoma cells; HeLa, *Homo sapiens* cervix; melanocytes, murine amelanotic melan-c melanocytes; NBD, *N*-(4-nitrobenzo-2-oxa-1,3-diazole); NBD-OPPC, 1-oleoyl-2-[6-[(7-nitro-2–1,3-benzoxadiazol-4-yl)amino]hexanoyl]-*sn*-glycero-3-phosphocholine; TR-DPPE, *N*-(Texas Red)-1,2-dipalmitoyl-*sn*-glycero-3-phosphoethanolamine; TRITC, *N*-(6-tetramethylrhodaminethiocarbamoyl); QD-DHPTE, quantum dot-conjugated 1,2-dipalmitoyl-*sn*-glycero-3-phosphothioethanol; Atto647N-PE, *N*-(Atto647N)-1,2-dipalmitoyl-*sn*-glycero-3-phosphoethanolamine.

[b]3T3-B, BALB/c 3T3 fibroblasts; C3H, mouse embryo fibroblasts; CHO-B1, CHO-K1 (Chinese hamster ovary) cells transfected with murine Fcγ receptor II type B1, called CHO-B1 (Miettinen et al. 1989, 1992); COS-7, SV40-transformed African green monkey fibroblasts; DLPC, 1,2-dilauroylphosphotidylcholine; DMPC, 1, 2-dimyristoyl-*sn*-glycero-3-phosphocholine; DOPC, 1,2-dioleoyl-*sn*-glycero-3-phosphocholine; DPPC, 1,2-dipalmitoyl-*sn*-glycero-3-phosphocholine; GUV, giant unilamellar vesicle; HASM, human coronary artery smooth muscle; KMSV-3T3, Kirsten murine sarcoma virus-transformed 3T3-B fibroblasts; NRK, normal rat kidney fibroblasts; POPC, 1-palmitoyl-2-oleoyl-*sn*-glycero-3-phosphocholine; POPE, 1-palmitoyl-2-oleoyl-*sn*-glycero-3-phosphoethanolamine; PS, bovine brain phosphatidylserine; PtK2, rat kangaroo normal kidney; SAINT-2, 1-methyl-4,19-*cis*, *cis*-heptatritiaconta-9,28-dienylpyridinium chloride; SPB, supported phospholipid bilayer; PtK1, rat kangaroo normal kidney.

[c]FCS, fluorescence correlation spectroscopy; FRAP, fluorescence recovery after photobleaching; FRAPP, fluorescence recovery after pattern photobleaching; NMR, nuclear magnetic resonance; NSOM, near-field scanning optical microscopy; SFD, single-fluorescent-molecule detection (epifluorescence); SFMT, single-fluorescent-molecule tracking; SPT, single-particle tracking; STED, stimulated emission depletion.

[d]Unknown acyl chains.

[e]NBD-PC, 1-palmitoyl-2-[-6[{7-nitro-2–1,3-benzoxadiazol-4-yl}amino]caproyl]-*sn*-glycero-3-phosphatidylcholine.

[f]D was estimated on the basis of the analysis assuming the presence of no immobile fraction.

[g]Fluctuation (noise) of the coordinates determined for Cy3-DOPE molecules attached to the coverslip (immobile control) gave the nominal diffusion coefficients in the range between 3.0×10^{-4} and 5.9×10^{-3} $\mu m^2\ s^{-1}$. Meanwhile, all fluorescent spots observed in these studies exhibited diffusion coefficients greater than 5.9×10^{-3} $\mu m^2\ s^{-1}$, and thus it was concluded that the mobile fraction was 100%.

[h]These SDs include, in addition to the experimental error, the true variations in the diffusion coefficient for individual molecules.

[i]Standard error.

[j]Time required for half of the observed fluorescence recovery to occur, read-off from the published recovery curves.

[k]Half-time of the total observation period after pattern photobleaching.

[l](Range of) diffusion time τ_d (defined by the lag time at half-maximum autocorrelation value) used to estimate D.

[m]Time required for half of the observed fluorescence recovery to occur (K. Jacobson, personal communication).

Table 2 Comparison of diffusion coefficients (D) for the same (or similar) membrane proteins between artificial versus cellular plasma membranes[a]

Probe[b]	Membrane type[c]	Method[d]	Mobile fraction (%)	D mean (±SD) ($\mu m^2\ s^{-1}$)	Time window for D (ms)	Temperature (°C)	References
Fl-AchR	100% DMPC	FRAP	>95	2.4 (±0.8)	2,600	36	Vaz et al. (1982)
Rh-AchR	*Rat Myotube*	*FRAP*	*75*	*0.016 (±0.003)*	*44,000*	*37*	Axelrod et al. (1976)
Alexa488-AchR	*CHO-K1/A5*	*FRAP*	*56*	*0.0,046 (±0.0,009)*	*~150,000*	NA	Baier et al. (2010)
Alexa488-AchR	*CHO-K1/A5*	*FCS*	*100*	*0.053 (±0.004)*	*~200*	NA	Baier et al. (2010)
Fl-Glycophorin[e]	100% DMPC	FRAP	85~98	2	3,000	30	Vaz et al. (1981)
Fl-Glycophorin[e]	100% DMPC	FRAP	85~98	4 (±2)	1,500	30	Kapitza et al. (1984)
Fl-Glycophorin[f]	*Erythrocyte (intact)*	*FRAP*	*56*	*0.0,036 (±0.0,017)*	*100,000*	*37*	Golan et al. (1986)
Fl-Glycophorin[f]	*Erythrocyte (ghost)*[g]	*FRAP*	*98*	*0.047 (±0.021)*	*10,000*	*37*	Golan et al. (1986)
Fl-Band3	100% DMPC	FRAP	98	1.6 (±0.4)	600	30	Chang et al. (1981)
Eo-Band3	*Erythrocyte (ghost)*[g]	*FRAP*	*41~83*	*0.0,046~ 0.065*	*21,000~ 43,000*	*37*	Golan & Veatch (1980)
Fl-Band3	*Erythrocyte (ghost)*[g]	*FRAP*	*40*	*0.60 (±0.069)*	*26,000*	*26*	Tsuji & Ohnishi (1986)
QD-Band3	*Erythrocyte (intact)*	*SPT*	*76*	*0.0,014 (±0.0,004) [77%] 0.022 (±0.01) [23%]*	*~8*	*37*	Kodippili et al. (2009)

[a]Cellular plasma membranes indicated by italics.
[b]Eo-Band 3, Eosin-labeled band 3; Fl-, Rho-, and Alexa488-AchR, fluorescein-, tetramethylrhodamine-, and Alexa488-labeled bungarotoxin bound to acetylcholine receptor, respectively; Fl-Band3, FITC-labeled band 3; QD-Band3, quantum dot–labeled band 3.
[c]CHO-K1/A5, a clonal cell line that stably expresses heterologous adult murine muscle-type AchR (Roccamo et al. 1999); DMPC, 1,2-dimyristoyl-*sn*-glycero-3-phosphocholine.
[d]FCS, fluorescence correlation spectroscopy; FRAP, fluorescence recovery after photobleaching; SPT, single-particle tracking.
[e]Fl-Glycophorin, FITC-labeled glycophorin.
[f]Fl-Glycophorin, fluorescein-thiosemicarbazide-labeled glycophorin.
[g]The amount of the spectrin network (erythrocyte membrane skeleton) remaining after the preparation of ghost membrane varies depending on the method and the stability of the spectrin skeleton in the ghost membrane depends on the ionic concentration of the medium used for each measurement. Therefore, the diffusion coefficients of transmembrane proteins vary greatly, depending on experimental conditions. Nevertheless, the tendency is for the diffusion coefficient to increase by ghost-membrane preparation, which partially removes spectrin.

indicate that any theory for predicting the diffusion coefficient in the plasma membrane must include the effect of the actin filaments and that the application of most previous theories must be limited to only simple Singer-Nicolson-type membranes, such as artificial reconstituted membranes, liposomal membranes, and the blebbed plasma membranes (Gambin et al. 2006, Saffman & Delbrück 1975; Note that the method described in the former paper is better for predicting the free-diffusion rates of solutes with sizes comparable to lipid, whereas the method described in the latter paper predicts them better for larger solutes. However, the application of both methods should be limited to free diffusion in simple membranes).

A decrease by a factor of 20 could not be explained by combining the effects of the crowding of membrane proteins (Peters & Cherry 1982, Frick et al. 2007, Vaz et al. 1982) and the presence of cholesterol (Dietrich et al. 2001, Lindblom et al. 1981). Note that, in blebbed membranes, the concentrations of integral membrane proteins and cholesterol remain the same, if the blebbing is performed appropriately.

This concept of the membrane-skeleton-induced decrease in the diffusion coefficient of membrane molecules is totally consistent with the data obtained in the erythrocyte membrane, where the spectrin meshwork forms the membrane skeleton underneath its plasma membrane. Sheetz et al. (1980) found that the diffusion coefficient of a TM protein, band 3, in the mouse erythrocyte mutant lacking the spectrin network is an order of magnitude greater than that in the normal erythrocyte, suggesting that the membrane skeleton interferes with the diffusion of membrane proteins. Furthermore, drug-induced enhancement of tetramers (versus dimers) of the spectrin (i.e., enhanced membrane-skeletal network) in erythrocyte ghost membranes significantly decreased the lateral diffusivity of band 3 in the plasma membrane, without affecting its rotational (reorientational) diffusion, suggesting that the collision of the cytoplasmic domain of band 3 with the membrane skeleton (spectrin tetramers) is primarily responsible for reducing the translational diffusivity of TM proteins (Tsuji & Ohnishi 1986, Tsuji et al. 1988).

THREE-DIMENSIONAL STRUCTURE OF THE CORTICAL ACTIN FILAMENT MESHWORK ON THE CYTOPLASMIC SURFACE OF THE PLASMA MEMBRANE

A typical electron micrograph of the cytoplasmic surface of the plasma membrane, prepared with minimal intrusion by using a rapid-freeze, deep-etch technique, is shown in **Figure 2*a*** (Morone et al. 2006). The filamentous mesh-like structures are the membrane skeleton. Because almost every filament exhibited a distinct striped pattern with a 5.5-nm periodicity, which is a characteristic signature of actin filaments (inset in **Figure 2*a***), the membrane skeleton largely consists of actin filaments. Furthermore, the image clearly demonstrates that the membrane skeleton entirely covers the cytoplasmic surface of the plasma membrane, except for certain membrane domains, such as clathrin-coated pits and caveolae (although these structures extensively interact with actin filaments). Electron tomography of these plasma membrane specimens has provided three-dimensional structures of the actin-based membrane skeleton. Using the three dimensional data, it was found that many actin filaments were located within 0.8 nm from the cytoplasmic surface of the plasma membrane, thereby defining the membrane areas surrounded by the actin filament meshwork. The size of each mesh structure was measured; its distribution is provided in the histogram shown in **Figure 2*b***.

MEMBRANE-SKELETON FENCE MODEL: HOP DIFFUSION OF TRANSMEMBRANE PROTEINS DETECTED BY HIGH-SPEED SINGLE-MOLECULE TRACKING

To understand the exact mechanism by which the actin-based membrane skeleton reduces the

diffusion coefficient in the plasma membrane by a factor of 20, high-speed single-molecule imaging was combined with a statistical analysis for each single-molecule trajectory. This single-molecule observation method revealed that virtually all the examined TM proteins in every cell type undergo a particular kind of motion (**Figure 3*a***). The motion is characterized by temporary confinement of the molecule in a bounded region of the membrane, with an average diameter of 40–300 nm interrupted by rare hops (1–50 ms) into adjacent, yet still temporarily confining, regions, which we call compartments (Kusumi et al. 1993, Sako & Kusumi 1994, Suzuki et al. 2005, Umemura et al. 2008). However, note that the older reports tend to overestimate the residency time within a compartment, which should be corrected according to the method developed by Fujiwara et al. (2002) and Murase et al. (2004). This behavior is termed hop diffusion, as the membrane molecules undergo macroscopic diffusion by hopping between adjacent compartments, although they diffuse freely within a compartment. In contrast, they exhibit only fast simple-Brownian diffusion in blebbed membranes.

For classification of single-molecule trajectories into simple-Brownian, suppressed, and directed diffusion modes, a general statistical method has been developed (Kusumi et al. 1993, also see figure 4 and its related text in Suzuki et al. 2005 for the statistical analysis of trajectories and hop-confined diffusion). Note that this classification is independent of the diffusion model (many scientists have misunderstood this point, and some still do). It simply determines whether the given trajectory has a $<5\%$ probability of being classified into the simple-Brownian diffusion mode, and if this is true, then the trajectory is classified into either the suppressed or directed diffusion mode. Also note that every compartment in **Figure 3** has been detected by a computer program (Fujiwara et al. 2002, Kusumi et al. 2005; the compartment detection software was used for only the trajectories classified into the hop-confined diffusion mode). The TM protein hop diffusion, which was initially surprising, was objectively deduced. Theoretical treatments of such hop diffusion have been developed by Powles et al. (1992), Niehaus et al. (2008), Kenkre et al. (2008), Kalay et al. (2008), and Novikov et al. (2011).

Note that slow-speed single-molecule imaging cannot detect such hop diffusion. The frame rates of the employed camera must be much higher (usually more than a factor of 40) than the hop frequency (Kusumi et al. 2010). Such hop diffusion was strongly influenced by modulating the interaction between the cytoplasmic domain of the TM protein and the actin-based membrane skeleton. In blebbed membranes, only fast simple-Brownian diffusion was observed, with a median diffusion coefficient of $\sim 5\ \mu m^2\ s^{-1}$, which is approximately 25-fold greater than that in the intact plasma membrane ($\sim 0.2\ \mu m^2\ s^{-1}$) (Suzuki et al. 2005). The hop diffusion was sensitive to actin-depolymerizing drugs (also see Lenne et al. 2006). [Because these drugs induce complex consequences depending on the cell type, the drug treatment duration, and the types and concentrations of drugs used, caution must be exerted when interpreting these data, particularly when macroscopic diffusion measurements are made (see Crane & Verkman 2008, Frick et al. 2007, Lommerse et al. 2006, Nishimura et al. 2006, Schmidt & Nichols 2004, Umemura et al. 2008, Vrljic et al. 2002).] With a reduction in the cytoplasmic length of the TM protein, the residency time within a compartment and the force needed to drag TM proteins across the compartment boundaries using an optical trap were decreased. The compartment boundaries were found to be elastic (Kusumi & Sako 1996, Kusumi et al. 2005). When the membrane skeleton was dragged by optical tweezers along the plasma membrane, the TM proteins undergoing diffusion (i.e., those that did not bind to the membrane skeleton) followed the movement of the membrane skeleton (Tomishige et al. 1998). In addition, the mesh size of the spectrin membrane-skeleton in the human erythrocyte evaluated by atomic force microscopy (Takeuchi et al. 1998) agreed well with the compartment

size sensed by band 3 (Tomishige et al. 1998).

Based on these findings, the membrane-skeleton fence model was proposed (**Figure 4*a*,*b***) (Kusumi & Sako 1996, Sako & Kusumi 1994). TM proteins protrude into the cytoplasm, and as shown in this model, their cytoplasmic domains collide with the actin-based membrane skeleton (**Figure 2*a***), which induces temporary confinement or corralling of TM proteins in the membrane skeleton mesh. TM proteins can hop between adjacent compartments when the distance between the meshwork and the membrane becomes large enough, or when the meshwork temporarily and locally dissociates. Tomishige et al. (1998) found that the latter effect is more important.

Cytoplasmic signaling molecules anchored to the inner surface of the plasma membrane by lipid chains also exhibited confinement within actin-based compartments (Ehrlich et al. 2004, Lommerse et al. 2005, Schaaf et al. 2009). Recently, the involvement of membrane-attached microtubules in forming polarized, elongated compartments with much larger sizes was reported (Jaqaman et al. 2011).

ANCHORED TRANSMEMBRANE PROTEIN PICKET MODEL: HOP DIFFUSION OF PHOSPHOLIPIDS DETECTED BY ULTRAHIGH-SPEED SINGLE-MOLECULE TRACKING

What about phospholipids, which are the most basic molecular species for membrane formation? Fujiwara et al. (2002) demonstrated that phospholipids, even those located in the outer leaflet of the plasma membrane, unexpectedly undergo hop diffusion between compartments with sizes similar to those detected by protein hop diffusion (**Figure 4*b***). The characteristic time for lipid residency within a compartment is generally shorter than that for TM proteins (1–10 ms). Therefore, the membrane compartments for lipids could not be detected until the development of ultrafast methods for performing single-particle tracking. Fujiwara et al. (2002) performed their measurements at a rate of 40,000 frames s^{-1} (25-μs resolution), the fastest single-molecule tracking ever made. The diffusion coefficient within a compartment is between 5 and 10 $\mu m^2\ s^{-1}$, which is comparable to the diffusion coefficients both in the blebbed membrane, where phospholipids undergo simple-Brownian diffusion ($\sim$8 $\mu m^2\ s^{-1}$), and in artificial membranes (**Table 1**).

When the membrane skeleton was modulated in various ways, the movement of phospholipids, even those located in the outer leaflet, was affected. The removal of the extracellular matrices and the extracellular domains of the membrane proteins, and the modulation of cholesterol-enriched raft domains hardly affected hop diffusion. Furthermore, phospholipids and TM proteins exhibited the same compartment size for the same cell type, although the residency times within a compartment were different (Suzuki et al. 2005). These results are very surprising, because the membrane skeleton is located on the cytoplasmic surface of the plasma membrane and cannot directly interact with the phospholipids located in the outer leaflet of the plasma membrane.

The distribution of the compartment sizes evaluated from the phospholipid diffusion was compared with that of the mesh sizes of the actin filaments on the plasma membrane, as determined by electron tomography (**Figure 2*b***). These two histograms agree reasonably well for cells within the same cell lines of both normal rat kidney fibroblasts and fetal rat skin keratinocytes, whereas the distributions differ greatly for different cell lines. These results strongly indicate the involvement of the actin-based membrane skeleton in the temporary confinement of phospholipids.

To provide an explanation for all these results related to the hop diffusion of phospholipids, which should be consistent with the hop diffusion of TM proteins, we proposed the anchored TM–protein picket model. According to this model, various TM proteins are anchored to and aligned along the membrane skeleton, and they effectively act as rows of pickets against the free diffusion of

phospholipids (**Figure 4*c***). This action is due not only to the steric hindrance effect of these picket proteins (Saxton 1987, 1990), but also to their hydrodynamic friction-like effects on the surrounding lipid molecules. The latter effect was first described for the membrane by Hammer's group (Bussell et al. 1994, 1995a, 1995b; Dodd et al. 1995). When a TM protein is anchored to the membrane skeleton and immobilized, the viscosity of the fluid around it (**Figure 4*d***) becomes higher as a result of the hydrodynamic friction effects at the surface of the immobilized protein. For example, consider a fluid running in a tube. The velocity of the fluid is smaller near the wall than it is in the center owing to the friction at the surface of the immobile wall. In **Figure 4*d***, a similar effect is pictured as being induced on the molecular scale at the surface of an immobile molecule. The viscosity is enhanced; thus, the diffusion of the membrane molecules is slowed down. Therefore, when many similarly anchored TM-protein pickets are aligned along the membrane-skeleton fence, the compartment boundary would become difficult for membrane molecules to traverse. In other words, by this view the plasma membrane is likely partitioned by TM-protein pickets lining the membrane-skeleton fence (Fujiwara et al. 2002, Kusumi et al. 2005). Model calculations and simulations suggested that an occupancy of only one-fifth to one-third of the boundary by protein pickets would be sufficient to induce the temporary trapping of lipids within a compartment and that proteins that are immobilized for as short as ~10 μs at a time can work as effective pickets. In the absence of a hydrodynamic friction effect, the steric hindrance of the pickets alone is insufficient to induce the temporary confinement of lipid molecules (Nicolau et al. 2006, 2007). The effect of the TM-protein pickets is related to the concept of the boundary lipids. For extensive discussions of the boundary lipids, readers are referred to Kusumi et al. (2004) and Kusumi et al. (2011).

Consistent with the picket model, de Monvel et al. (2006) found that lipid diffusion is faster in the axial direction of the cell along the polarized membrane skeleton than it is in the circumferential direction, in cochlear outer hair cells where the membrane skeleton in polarized. Many reports support the hop diffusion of lipids (for example, Boucrot et al. 2006, Murcia et al. 2008, Saxton 2007).

ANSWERS TO THE 30-YEAR-OLD ENIGMA: THE PARTITIONING OF THE PLASMA MEMBRANE (COMPARTMENTS) DISTINGUISHES IT FROM THE SIMPLE SINGER-NICOLSON MEMBRANE

Our results show that each molecule in the plasma membrane exhibits two diffusion coefficients. One is for diffusion within a compartment (which we call the microscopic diffusion coefficient) and its value is 5–10 $\mu m^2\ s^{-1}$, which is comparable to that in artificial membranes and in blebbed plasma membranes. The other is for the macroscopic diffusion across many compartment boundaries, which is 0.2–0.5 $\mu m^2\ s^{-1}$, and is consistent with the macroscopic diffusion coefficients previously found in the plasma membrane as well as with those found in slow-speed single-molecule tracking. Note the factor-of-20 difference here. This explains the 30-year-old enigma, i.e., the difference in the diffusion coefficient by a factor of 20 between the plasma and artificial membranes. Previous measurements were all made in space scales greater than 500 nm. Therefore, in the case of the plasma membrane, they represented only the macroscopic diffusion coefficient across many compartments, which is ~20-fold slower than that found in artificial membranes (where the long-term diffusion rate is the same as the short-term diffusion rate). However, the microscopic diffusion coefficient within a compartment in the plasma membrane can now be measured, and results indicate that it is as large as that in artificial membranes (as well as in the blebbed membrane).

Given these and many other observations, we reached the following conclusion: The

Singer-Nicolson model is perfectly suitable for quantitatively describing the molecular events occurring in space scales of approximately 10 nm (~10% area in the smallest compartments found thus far) in the plasma membrane. However, for greater scales, to exactly understand molecular diffusion and reaction, the partitioning of the plasma membrane by the actin-based membrane skeleton fence and its associated TM-protein pickets must be considered. Because such partitioning of the plasma membrane has been found in all the cells examined to date, we consider the partitioning of the plasma membrane to be universal. Therefore, we propose that a paradigm shift for the long-range (>10 nm) structure of the plasma membrane is required: from the two-dimensional continuum fluid model of Singer and Nicolson to the compartmentalized fluid model, in which membrane molecules undergo short-term confined diffusion within a compartment and long-term hop diffusion between the compartments. The partitioning of the plasma membrane (compartments) by fences and pickets, which results in the observed hop diffusion of membrane molecules, makes the plasma membrane distinct from the simple Singer-Nicolson membrane. Thus, we consider the compartmentalization of the plasma membrane to be the first tier of the hierarchical mesodomain architecture of the plasma membrane.

How did it become possible to identify the hop diffusion of membrane molecules in the partitioned plasma membrane, which had gone undetected for more than 30 years after Singer & Nicolson (1972)? First, single-molecule observations had to be used. In effect, if more than one molecule is observed at a time, then the individual hop events will be masked by the averaging over all molecules under observation. Second, high-speed or high-time-resolution observations were another key factor. The confinement within the domain can be detected only when sufficient numbers of observations are made during the residency time within a domain or a compartment. Because the residency time is usually between 1 and 40 ms, the time resolution must generally be better than 0.025 ms. Therefore, hop diffusion cannot be detected by slow-speed single-molecule imaging (Crane & Verkman 2008, Kusumi et al. 2010, Lommerse et al. 2006, Vrljic et al. 2005, Wieser et al. 2007).

Other mechanisms for solving this enigma have been considered. The effects of cholesterol or the crowding of membrane proteins could explain a 20% difference, but never a 20-fold difference, even if they are combined. Although unlikely, the presence of membrane protrusions and dips could cause apparent confinement (Adler et al. 2010). To reduce the macroscopic diffusion coefficient by a factor of 10, the protrusions or dips must be as large as 100–300 nm for a compartment size of 200 nm and they must be present throughout the cell membrane. This is clearly inconsistent with the electron microscopy observations (with the possible exception of the brush-border membranes of epithelial cells) (Morone et al. 2006, Rothberg et al. 1992). It is also inconsistent with most of the observations that led to the proposal of the membrane-skeleton fence model (see the previous section on Membrane-Skeleton Fence Model).

A COMPARTMENTALIZED VIEW OF THE PLASMA MEMBRANE IS ESSENTIAL FOR UNDERSTANDING ITS FUNCTION: THE MEMBRANE MECHANISM BASED ON THE MEMBRANE-SKELETON-INDUCED COMPARTMENTS

The fundamental influence of the actin-based membrane skeleton on the molecular dynamics and structure of the membrane suggests that, to understand the mechanisms of any plasma membrane function, including signal transduction, the effect of the actin-induced partitioning of the plasma membrane or the first-tier mesoscale compartments must always be considered. Any interpretation and modeling based on the experimental results on the dynamics, oligomerization, and domain

formation of membrane-associated molecules must consider and be consistent with the effect of the actin-based compartmentalization of the plasma membrane. The models based on observations made in simple artificial membranes, in the absence of associated actin filaments, cannot be directly used to interpret the experimental results obtained in the plasma membrane in space scales greater than ~10 nm (if the experiment addresses the question relevant to the dynamics and structure within 10 nm and is not directly coupled to the actin-membrane skeleton, then this statement will not apply). A 20-fold difference in the macroscopic diffusion coefficient is too large to be neglected. Furthermore, this factor will become much greater than 20 when the membrane molecules form oligomers (see the later section on Oligomerization-Induced Trapping). In the following five subsections, we discuss functions of actin-membrane-skeleton-induced compartments.

Regulating Receptor Distributions and Interactions for Signal Transduction Functions

Receptor redistribution and clustering are key steps in many signal transduction pathways (Briegel et al. 2009, Minguet et al. 2007, Nikolaev et al. 2010, Petrini et al. 2004). Several reports have indicated the active roles played by the cytoskeleton in inhibiting (Boggs & Wang 2004, Wang et al. 2001) or enabling (Baumgartner et al. 2003, Gomez-Mouton et al. 2001, Rodgers & Zavzavadjian 2001) the redistribution/clustering of membrane molecules.

In B cell–receptor regulation, the confinement of the receptor within actin-membrane-skeleton-induced compartments is an important mechanism for suppressing the B cell–receptor diffusivity and the autoactivation of the B cell–receptor signaling in steady-state cells before stimulation (Treanor et al. 2010). This study further suggested that ezrin plays an important role in connecting the actin cytoskeleton to the TM-protein pickets on the membrane skeleton. Upon antigen binding, B cell receptors form closely associated oligomers (Fleire et al. 2006, Liu et al. 2010, Pierce & Liu 2010, Tolar et al. 2005) in a manner dependent on cortical actin reorganization mediated by Rac2-Rap1 signaling (Arana et al. 2008, Lin et al. 2008).

The epidermal growth factor receptor (EGFR) is more concentrated and, therefore, more readily able to form steady-state oligomers as well as liganded oligomers near the peripheries of the cell where the actin-membrane skeleton is more extensively developed and apparently has smaller meshes (Chung et al. 2010). Increasing the receptor's local concentration, and thereby facilitating oligomer formation, may be the most important functions of the membrane compartmentalization by the membrane skeleton.

In addition to the actin-membrane skeleton, the extracellular galectin-3 lattice may provide another mechanism for impeding the diffusion of glycoproteins. Lajoie et al. (2007) showed that EGFR diffusion is suppressed by the interaction of its N-glycans with the galectin-3 lattice. The slowing of EGFR diffusion by these two structures predominantly protects EGFR from loss to oligomerized-caveolin1 microdomains containing ~15 caveolin1 molecules and caveolae, where EGFR signaling is suppressed (Parton & Simons 2007, Parton et al. 2006). Therefore, the balance between these regulation instruments will be important for promoting cell growth as well as suppressing tumors. Arguments have been advanced that a similar mechanism may function to control cell-substrate adhesion (Gaus et al. 2006, Lajoie et al. 2009).

Kv2.1 potassium channels form dynamic "clusters," with sizes and spatial distributions that are influenced by the actin-based membrane skeleton (O'Connell et al. 2006). Interestingly, the individual channels diffused freely within a cluster, suggesting that the clusters may not be real molecular oligomers but instead function as channel molecules that are corralled by the membrane skeleton. This proposal was further supported by the results obtained upon membrane skeleton disruption by latrunculin A

treatment, which resulted in a 10-fold increase in the average cluster area and a decrease in the number of clusters, indicating that the smaller clusters merged during the treatment. Furthermore, in cells with an intact cytoskeleton, the Kv2.1 channels were restricted to the cell body. However, after latrunculin A treatment, the channels were found in the neurites as well as in the cell body. These observations suggest that the Kv2.1 clusters are maintained in the membrane skeleton–based domains and that an actin-based mechanism is involved in determining the spatial distribution of Kv2.1 channels.

Oligomerization-Induced Trapping for Receptors

Receptor monomers can hop across the intercompartment boundaries quite readily, but when they form oligomers upon liganding, the hop rate decreases dramatically as a result of the increased size (**Figure 5**). In addition, owing to the avidity effect, molecular complexes are more likely to be bound to the membrane skeleton. Such enhanced confinement and binding of receptor oligomers are collectively termed oligomerization-induced trapping (Iino et al. 2001, Kusumi & Sako 1996, Kusumi et al. 2005). Therefore, oligomerization or protein-complex formation is tied to longer confinement within the compartment where the receptor oligomers are initially formed. Specifically, the third and first tiers in the hierarchical architecture are well coupled for membrane functions. Without membrane compartmentalization, oligomerization alone cannot slow receptor diffusion to such an extent (Kusumi et al. 2011, Liu et al. 1997, Peters & Cherry 1982, Saffman & Delbrück 1975, Vaz et al. 1982).

For example, the FcεRI receptor, which can be activated by crosslinking with a multivalent antigen, becomes immobilized within seconds of crosslinking, and disruption of the actin cytoskeleton results in delayed immobilization kinetics and increased diffusion of crosslinked clusters, in accordance with oligomerization-induced trapping (Andrews et al. 2008). These results suggest that actin-induced membrane partitioning dynamically influences both the receptor sequestration and response to ligand binding. A number of other publications have reported that oligomerization-induced trapping occurs and plays important functional roles in various plasma membrane processes (for example, see Carramusa et al. 2007, Cavey & Lecuit 2009, Chien et al. 2009, Fu et al. 2008, Moerner 2002). Therefore, it is concluded that the engaged receptors that form oligomers are trapped within/around the compartment (or bound to the compartment-forming actin skeleton) where the signal was received initially by the receptor. Such localized signal sources would remain within the compartment longer, providing the effect of the short-term memory for the place where the signal was received, and would be important for local or polarized responses of the cell, such as chemotaxis.

Creating Macroscopic Diffusion Barriers

The third function of the membrane-skeleton fences and associated pickets may be to form macroscopic diffusion barriers in the plasma membrane. The size of the barrier could be on the order of several tens of nanometers to tens of microns. The presence of various macroscopic diffusion barriers in plasma membranes has been reported. Some of them may be selective molecular species barriers. Representative macroscopic diffusion barriers are found in the plasma membrane of the following regions of the cell: the neuronal initial segment/axon hillock, located at the base of the axon (interfacing with the cell body) (Kobayashi et al. 1992, Nakada et al. 2003, Nishimura et al. 2006, Winckler et al. 1999; but see Boiko et al. 2007, Brachet et al. 2010, Winckler & Poo 1996), the intercompartmental boundaries in neurites (Katsuki et al. 2011), the boundaries located between three different regions in spermatozoa (Arts et al. 1994, Cowan et al. 1987, Ihara et al. 2005, Kwitny et al. 2010), the node of dendrite branching in spine morphogenesis (Tada et al. 2007, Xie et al. 2007), the base of the cilium in the epithelial cell (Francis et al. 2011,

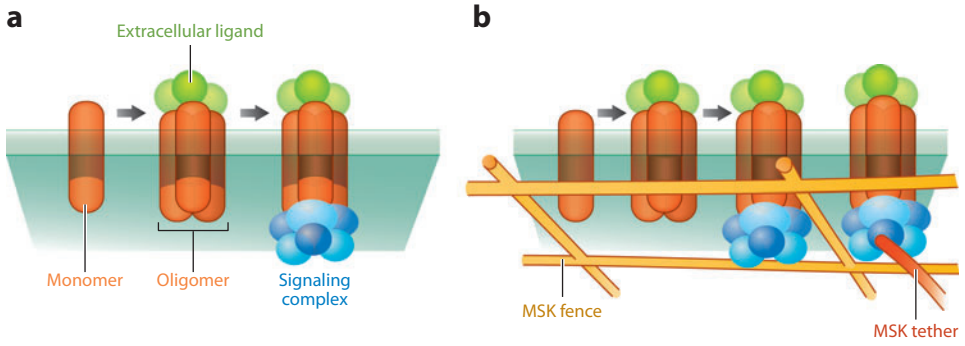

Figure 5

Schematic representation of oligomerization-induced trapping. (*a*) In the absence of fences and pickets, oligomerization alone induces only slight decreases in the diffusion coefficient. (*b*) Only in the presence of fences and pickets can oligomerization significantly reduce diffusion rates. Abbreviations: MSK, membrane skeleton

Hu et al. 2010, Nachury et al. 2010), and the bud neck of yeast (Takizawa et al. 2000), as well as the cleavage furrow of dividing mammalian cells (Schmidt & Nichols 2004) (**Figure 6**). The septin polymers bound to the plasma membrane may be responsible for the latter five diffusion barriers (Caudron & Barral 2009).

The diffusion barrier located at the neuronal initial segment membrane works for both phospholipids and TM proteins. The barrier is generated by a massive assembly of various TM proteins and actin-related membrane-skeletal proteins. These proteins bind to each other in the initial segment region of the membrane, in a phenomenon occurring between days 5 and 10 after birth, in the case of rat hippocampal neurons. Very dense rows of anchored-protein pickets and/or rows with high densities of pickets are formed, practically blocking the macroscopic diffusion of phospholipids in the initial segment membrane (Nakada et al. 2003). Other macroscopic diffusion barriers may also be formed via the binding of various TM-protein pickets to the membrane skeleton, although the membrane-skeletal protein responsible for the barrier formation may vary in different cell types and barriers.

A different type of macroscopic diffusion barrier exists in the oligodendrocyte myelin membrane, which wraps around the axon. Because the myelin membrane must be enriched in lipids for insulation, the basic myelin protein forms a barrier that functions as a physical filter that restricts only protein diffusion by placing its large cytoplasmic domain into the myelin (Aggarwal et al. 2011).

Local Reaction Bursts in the Partitioned Plasma Membrane, Creating Spatiotemporal Variations of the Reaction Rate

Assuming an average compartment size of 60 × 60 nm and a flat cell of 60 × 60 μm, a single cell contains 2 million compartments. Meanwhile, the average copy number of receptors in the plasma membrane is typically on the order of 10^4–10^5 copies/cell (most receptors appear to be expressed in the range of 10^3–10^6 copies/cell) (see table 2-1 of Lauffenburger & Linderman 1993) or 1–15 copies/μm^2. Therefore, a receptor molecule exists in approximately every 20–200 compartments, which is quite sparse.

Under such sparse expression conditions, membrane compartmentalization/partitioning appears to pose a big dilemma. Although it might be useful for various membrane functions, because it slows the macroscopic diffusion rates by a factor of 20 on average, it

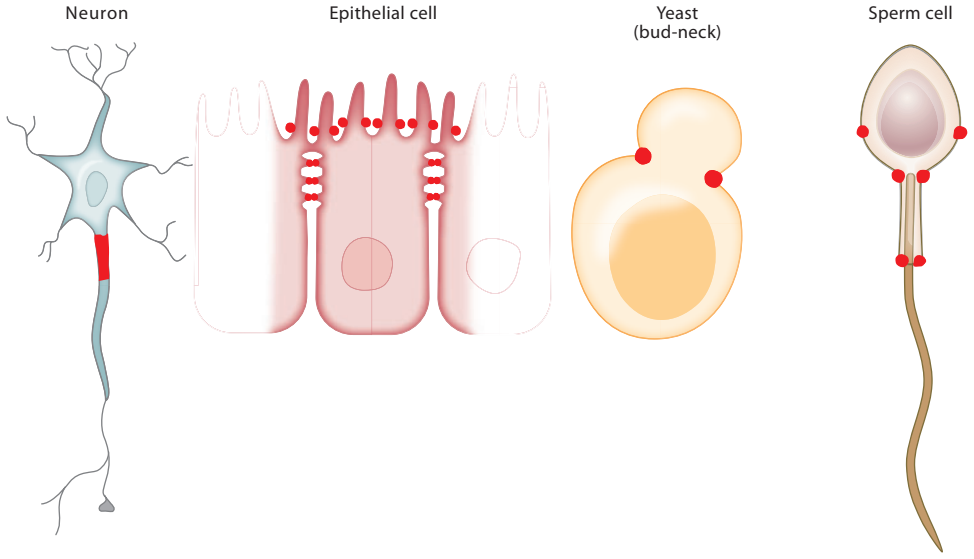

Figure 6

Representative macroscopic diffusion barriers, which we consider to be formed by the enhanced picket-fence effects.

may greatly reduce the bimolecular collision rates and thus tremendously retard the reaction rates in the plasma membrane. Meanwhile, thermodynamic considerations suggest that because the presence of semipermeable barriers in the plasma membrane does not affect the monomer-dimer equilibrium (thus reversible bimolecular reaction) in the plasma membrane, it should not affect the overall collision rate of membrane molecules averaged over the entire plasma membrane.

This problem was examined theoretically and computationally (Kalay et al. 2012). As predicted thermodynamically, even in the presence of membrane partitioning, the overall reversible bimolecular reactions (formation rates of dimers and monomers) in the entire membrane were found to occur at the same rate, except for extreme cases. In contrast, bimolecular reactions that occur in each compartment were found to proceed in bursts during which the reaction rate is sharply and briefly increased. Namely, it will take a long time before two molecules enter the same compartment, but once they enter the same compartment, they will collide very often within the compartment before one of them escapes from the compartment (same as the local concentration effect, Saxton 2002), greatly enhancing the number of collisions. Namely, actin-induced compartments are considered to create spatial variations in the reaction rate, without affecting the overall reaction rate. In at least one experiment, the oligomerization rate of the EGF receptor increased with an increase in the density of the actin-based membrane skeleton (Chung et al. 2010).

We believe that such localized enhanced reactions will be very important for signaling. Consider kinase activation. If weak kinase activation occurs throughout the plasma membrane, then phosphorylation will be eliminated by the strong phosphatase activities (Heinrich et al. 2002, Klarlund 1985, Lerea et al. 1989, Mocciaro & Schiebel 2010). However, if kinase activation occurs within a compartment, then it can create many phosphorylated downstream molecules within the compartment, and if a

specific phosphatase is absent in that compartment, then the phosphorylation signal in those compartments will survive, creating spatial patterns of activation.

The Actin-Based Membrane Skeleton May Work as a Base Scaffold

Many receptor and other membrane-associated molecules are often temporarily bound to actin filaments directly or indirectly by way of a third or more proteins (Bretscher 1999, Haggie et al. 2006), and this temporary binding is often enhanced upon receptor engagement. One of the clearest results of ligand-induced receptor binding to actin filaments would be the one found by Suzuki et al. (2007a,b). When a GPI-anchored receptor, CD59, was activated by crosslinking, the CD59 cluster, containing an average of six molecules, exhibited alternating periods of temporary immobilization (0.57 s), called stimulation-induced temporary arrest of lateral diffusion (STALL), and slow Brownian diffusion (1.2 s; observed as Brownian diffusion because the camera's frame rate was too slow to detect hop diffusion). STALL was induced via the binding of the CD59 cluster to the actin filament (by way of an as-yet-unknown protein), and only during the STALL period of CD59 clusters, PLCγ2 molecules were recruited at the CD59 clusters to trigger inositol triphosphate (IP_3)-Ca^{2+} responses. Thus, the temporary binding of CD59 clusters to the actin filament constitutes a key step for transducing the extracellular CD59 signal to the intracellular IP_3-Ca^{2+} signal.

The mechanisms for the STALLing of engaged receptors and its advantages in signal transduction are unknown. However, because immobilization will not provide any advantages for signal transduction, we believe it is a consequence of the interaction of the engaged receptor with actin-bound (directly or indirectly) scaffolding molecules that link the receptor to the downstream signaling molecule. In effect, the actin-based membrane skeleton could serve as a base scaffold for pooling and presenting cytoplasmic scaffolding/signaling proteins to membrane-associated molecules. Meanwhile, the formation of engaged receptor clusters may lead to de novo polymerization of actin filaments at the receptor cluster (Co et al. 2007) (**Figure 5**), thereby enhancing their interactions with the actin-based membrane skeleton and associated signaling and scaffolding molecules and/or triggering the large-scale reorganization of the actin cytoskeleton for polarized cellular responses. The interactions of receptors, signaling molecules and their scaffolding proteins bound to actin filaments, and actin filaments themselves would be critically important in organizing receptors and signaling molecules and regulating their functions (Gowrishankar et al. 2012). Clearly, more research on such interactions and their functional relevance is required.

THE SECOND TIER: MESOSCALE RAFT DOMAINS, COUPLED TO THE FIRST- AND THIRD-TIER MESODOMAINS

Owing to space limitations, the raft domains are here discussed almost exclusively in terms of their relationships with membrane-skeleton-induced compartments and dynamic protein complex domains, with a strong focus on how they contribute as membrane mechanisms to generating functions of the plasma membrane.

The Actin-Based Membrane Skeleton May Both Suppress and Enhance the Raft Growth over the Compartment Boundaries

The blebbed membrane, a balloon-like structure of the plasma membrane formed by removing the actin-based membrane skeleton (described above; see A Compartmentalized View of the Plasma Membrane Is Essential for Understanding Its Function) is often used in raft research, while it is still attached to the plasma membrane or after detaching, in the form of a giant unilamellar vesicle. When the temperature of the blebbed membrane was lowered to ~12°C (Baumgart et al. 2007) [or the GM1

ganglioside was crosslinked by cholera toxin (Kaiser et al. 2009, Lingwood et al. 2008)], the blebbed membrane exhibited two distinct domains greater than several microns in diameter, a much larger size than that of the membrane compartments formed by membrane partitioning (40–300 nm in diameter). These two domains were enriched in either raft or nonraft molecules and were probably induced by a mechanism analogous to phase separation (Baumgart et al. 2007). The formation of such micronscale domains was never observed in the presence of the intact actin-membrane skeleton (Baumgart et al. 2007). Therefore, the cold induction of these micronscale domains revealed (*a*) the capability of the plasma membrane to form raft domains as well as (*b*) the critical role of the actin-based membrane compartmentalization (with associated TM-protein pickets) in suppressing raft growth beyond the intercompartmental boundaries (**Figure 1**).

We believe that membrane compartments and raft domains, which constitute the first and second tiers in the hierarchy of mesoscale domains, respectively, coexist in the plasma membrane (Pralle et al. 2000, Viola & Gupta 2007) (**Figure 1**). Furthermore, GPI-anchored proteins undergo hop diffusion in exactly the same manner as phospholipids in response to the temporary confinement by the picket fence (Umemura et al. 2008). Note that the TM-protein pickets tend to exclude cholesterol from the first annulus in the membrane (Simmonds et al. 1982, Warren et al. 1975). This is due to the structural incompatibility between the bulky, rigid tetracyclic sterol backbone of cholesterol (Pasenkiewicz-Gierula et al. 1991; Subczynski et al. 1990, 1991) and the rough surface of the TM domains formed by the protruding side chains of various amino acids in the TM domain (Kusumi et al. 2004, Subczynski et al. 2003), making the compartment boundaries a very raft-unfriendly environment. In this way, the raft growth is considered suppressed by the intercompartment boundaries composed of the actin-based membrane skeleton and the associated TM-protein pickets, explaining the formation of large raft domains in blebbed membranes at lower temperatures (Baumgart et al. 2007, Kaiser et al. 2009, Lingwood et al. 2008). Simple lowering of temperature could not induce formation of micrometer-sized raft domains in the intact plasma membrane. Thus, the rafts are limited to sizes smaller than those of the compartments (40–300 nm in diameter, depending on the cell type). A more comprehensive discussion is provided by Kusumi et al. (2011).

Meanwhile, experimental and simulation investigations have revealed that the association of actin filaments and its meshwork with the membrane bilayer can enhance microdomain formation and subdiffusion (Ehrig et al. 2011, Garg et al. 2009, Lasserre et al. 2008). This may be further enhanced by binding the nanoclusters or stabilized rafts of GPI-anchored proteins to the membrane skeleton (Goswami et al. 2008, Suzuki et al. 2007b). In T cell–receptor signaling, the association of CD28, a coreceptor, with the actin-binding protein filamin A is essential to recruit the downstream Src-family kinase to the immunological synapse (Tavano et al. 2006). Chaudhuri et al. (2011) extended the investigation and theoretically/computationally showed that the active contractility and remodeling of the cortical actin filaments can induce transient focusing of GPI-anchored proteins and their clusters (as stated above, the clusters of GPI-anchored proteins can interact with actin filaments) to form larger clusters. Hence, the cortical actin filaments could induce dramatic increases in the reaction efficiencies and the signal output levels. These results indicate that ligand-induced larger rafts, generated by the clustering of engaged raft-associable receptors, can bind to the actin-membrane skeleton, possibly making their specific surrounding environment within the intercompartmental boundary region more raft friendly. Such ideas would be testable using high-speed single-molecule imaging techniques, combined with single- or multi-molecular methods for imaging signals (e.g., Murakoshi et al. 2004).

At the end of the section on membrane compartmentalization, the interaction of actin-based membrane skeleton with receptors, intracellular signaling molecules, and their scaffolding molecules was emphasized for their possible significance in signaling. Likewise, here, we emphasize the active roles that actin membrane skeleton might play in both suppressing and enhancing raft formation and raft-linked signal transduction.

The Coupling of Raft Domains and Dynamic Protein Complex Domains

Raft domains are distinguished from dynamic protein complexes by the involvement of lipid-lipid interactions in raft formation and the recruitment of molecules. The lipid interactions here include those involving lipids attached to proteins. However, for the specificity of signaling and protein transport, protein-protein interactions play key roles in the formation and function of raft domains, as exemplified by the signal transduction of CD59 and the dendritic cell LPS receptor CD14 (both are GPI-anchored receptors) (Suzuki et al. 2007a, 2007b; Zanoni et al. 2009) and in protein transport (Imjeti et al. 2011, Paladino et al. 2008; also see Hess et al. 2007, Kenworthy et al. 2004).

Protein-protein interactions are critical at four stages in the raft-based signal transduction of GPI-anchored receptors (Suzuki et al. 2007a,b; 2012): (*a*) in resting cells, where GPI-anchored receptors continuously form transient homodimers/oligomers, (*b*) when the ligand induces more stable homodimers/oligomers of GPI-anchored receptors, and (*c*) when raft-associable TM signaling/scaffolding proteins and/or (*d*) the cytoplasmic lipid-anchored signaling proteins are recruited to the induced homodimers/oligomers of GPI-anchored receptors. Note that, although raft-associable TM receptors, which are probably mostly palmitoylated (Levental et al. 2010), will behave in a similar manner to GPI-anchored receptors, for brevity here we use the term GPI-anchored receptors to represent any raft-associable receptors.

In the first step, which occurs in resting cells, virtually all of the GPI-anchored receptor molecules are mobile and continually form transient (~200 ms) homodimers through ectodomain protein interactions, stabilized by the presence of the GPI-anchoring chain and cholesterol (termed GPI-anchored protein homodimer rafts, or homodimer rafts for short). Heterodimers do not form, which suggests a fundamental role that the specific ectodomain protein homo interaction plays in the formation of GPI-anchored, repector-based raft domains (Suzuki et al. 2012). Under higher physiological expression conditions, homodimers coalesce by raft-based lipid interactions to form hetero- and homo-GPI-anchored receptor oligomer rafts or greater raft domains or nanoclusters of 5–20 nm in diameter (Parton & Hancock 2004, Sahl et al. 2010, Sharma et al. 2004). For the assembly of these greater raft domains (but still of the size of <20 nm), active processes involving actin filaments might be involved (Goswami et al. 2008, Suzuki et al. 2012).

In the second step, upon ligand binding, conformational changes of the ecto-protein domain would be induced, leading to the formation of the ligand-induced stabilized raft domains of homodimers/oligomers of GPI-anchored receptors, which would in turn be further stabilized by raft-lipid interactions (the key protein-protein interaction step; Suzuki et al. 2012). These homodimers/oligomers will serve as nuclei to assemble cholesterol and other saturated lipids (mostly glycosphingolipids), forming the homodimer/oligomer raft domains. This probably occurs cooperatively, like condensation. Raft-associable lipids might be considered at the homodimers/oligomers of GPI-anchored receptors in the bulk plasma membrane. The presence of transient homodimer rafts is likely to facilitate this process because they enhance and accelerate intracellular signaling. However, such induced raft domains do not seem to grow much more than the sizes of the initiating nuclei of homodimers/oligomers of liganded GPI-anchored receptors (Goswami et al. 2008; Sohn et al. 2006, 2008; Suzuki et al. 2007a,b). The induced homodimer/oligomer

rafts based on different GPI-anchored receptors then may form greater heterocomplexes as a result of raft lipid interactions, which could facilitate important cross talk between different signaling pathways (Chaudhuri et al. 2011, Goswami et al. 2008, Sharma et al. 2004).

In the third step, the induced homodimer/oligomer rafts of the liganded GPI-anchored receptor recruit (raft-associable) TM scaffolding/signaling proteins through the interaction of the ectodomain of the GPI-anchored receptor and the TM protein (protein-protein interactions) as well as the raft interactions between the two proteins. The recruitment of such TM proteins is needed to recruit the specific cytoplasmic signaling molecule to the engaged receptor, because GPI-anchored receptors extend only halfway through the membrane (Chen et al. 2009; Suzuki et al. 2007a,b). In the case of raft-associable TM receptors (such as Fcϵ, T cell, or B cell receptors), scaffolding TM proteins may not be necessary.

In IgE-receptor signaling, biochemical data suggest the raft-interaction-dependent recruitment of the lipid-anchored Src-family kinase Lyn to the engaged, clustered receptor, although its direct detection has been difficult (Field et al. 1997, Sheets et al. 1999). However, several lines of evidence suggest the transient recruitment of Lyn under normal stimulation conditions (Larson et al. 2005, Shvartsman et al. 2007, Wu et al. 2004).

In B cell–receptor signaling, the nanoclustering of the antigen-dependent, B cell–receptor-induced raft assembly (association with raft probes) and coligation of CD19 with the receptor prolonged both the raft association and interaction with Lyn (a direct downstream, raft-associated molecule) (Sohn et al. 2006, 2008). Interestingly, in T cell–receptor signaling, coligation/coclustering of CD3 and CD28 induced raft formation at their clusters, as shown by the assembly of GM1 and the lipid-anchoring peptide of Lck (GFP conjugated), whereas the ligation of only CD3 failed to do so (Tavano et al. 2006, Viola et al. 1999; but see Yokosuka & Saito 2009). However, such differences between T and B cell–receptor signaling may be due to the quantitative differences in the strengths of stimulation: The use of supported planar bilayers provides almost infinite supplies of the antigens, MHC proteins, and other stimulating proteins, versus the environment provided by the real antigen-presenting cells. Supported planar bilayers also provide the correct two-dimensional geometry, which strongly enhances the binding efficiency, also in contrast to the three-dimensional application of the antigens and other costimulating proteins, as reported by Huang et al. (2010) and Huppa et al. (2010). Note, however, that the involvement of a protein-based network formed upon stimulation has been suspected in T cell–receptor signaling (Douglass and Vale 2005, Dustin & Depoil 2011, Hartman & Groves 2011, Kaizuka et al. 2009, Yokosuka & Saito 2010). Readers should be aware that some of these observations proved causality, but some rather indicated interesting correlation (and some of them indicated very strong correlation).

Such signaling molecular complexes are transported to the immunological synapse in a dynein-dependent manner (Hashimoto-Tane et al. 2011). However, how can such transport occur in the presence of the actin-based membrane skeleton meshwork? Previous optical trapping experiments revealed that the membrane skeleton meshes continually undergo temporary dissociation (Tomishige et al. 1998) [originally proposed as the spectrin dimer-tetramer equilibrium gate model by Tsuji et al. (1988) and Sako et al. (1998)]. Therefore, if a molecular complex is slowly dragged along the plasma membrane (either by a motor protein or optical tweezers) against the membrane skeleton, then the membrane skeleton will likely dissociate before excess tension builds up between the dragged molecular complex and the membrane skeleton mesh and the molecular complex will pass through the open gate of the membrane skeleton (Tomishige et al. 1998). This is entirely consistent with the single-molecule force spectroscopy theory (Evans & Ritchie 1999, Merkel et al. 1999).

Therefore, dynein-dependent transport of the T cell–receptor clusters within the plasma membrane is consistent with the concept of the dynamic membrane skeleton fence.

THE THIRD TIER: DYNAMIC PROTEIN COMPLEX DOMAINS

The coupling of the third-tier dynamic molecular complex domains with the first- and second-tier mesodomains is discussed above. Although the cooperative actions of the three tiers are important for signal transduction by the plasma membrane, we do not discuss this further here owing to space limitations. Instead, the interested reader is referred to a complementary review including in-depth discussions on the second and third tiers and their relationships with the first-tier compartments (see Kusumi et al. 2011, 2012).

CONCLUSIONS

The low dimensionality (two dimensions compared with three dimensions) of the fluid plasma membrane is the key for efficient molecular collisions and subsequent reactions. In addition, the two-dimensional surface interfaced with the three-dimensional cytoplasmic space provides an important reaction field. Without such an enhancing mechanism, as one of the membrane mechanisms, plasma membrane functions would not be possible.

In addition to the mechanism for enhancing the basic collision/reaction rates, the plasma membrane is equipped with the mechanisms to regulate spatiotemporally the molecular collision rates and the durations of molecular interactions. In this review, we summarized these membrane mechanisms as those that are carried out by the cooperative action of three-tiered hierarchical dynamic organization of molecules in the plasma membrane: (*a*) partitioning of the entire plasma membrane via the actin-based membrane skeleton and the associated TM-protein pickets (first tier); (*b*) the metastable raft domains (Honerkamp-Smith et al. 2008) undergoing cooperative assembly and disassembly (second tier); and (*c*) the transient protein complex domains, including oligomers of integral membrane proteins, coat-protein-facilitated domains, and scaffolding-protein-induced protein complex domains (third tier). The basic molecular interactions required for the signal transduction function of the plasma membrane can be fundamentally understood and conveniently summarized as the cooperative actions of these three mesoscale domains in which thermal fluctuations/movements of molecules and weak cooperativity play crucial roles.

DISCLOSURE STATEMENT

The authors are not aware of any affiliations, memberships, funding, or financial holdings that might be perceived as affecting the objectivity of this review.

ACKNOWLEDGMENTS

We thank all of the members of the Kusumi lab for fruitful discussions and critical readings of this manuscript as well as Mr. Kohji Kanemasa for preparing the figures. This work was supported in part by Grants-in-Aid for Scientific Research from MEXT (A.K., K.G.N.S., R.S.K., and T.K.F.).

LITERATURE CITED

Adler J, Shevchuk AI, Novak P, Korchev YE, Parmryd I. 2010. Plasma membrane topography and interpretation of single-particle tracks. *Nat. Methods* 7:170–71

Aggarwal S, Yurlova L, Snaidero N, Reetz C, Frey S, et al. 2011. A size barrier limits protein diffusion at the cell surface to generate lipid-rich myelin-membrane sheets. *Dev. Cell* 21:445–56

Andrews NL, Lidke KA, Pfeiffer JR, Burns AR, Wilson BS, et al. 2008. Actin restricts FcεRI diffusion and facilitates antigen-induced receptor immobilization. *Nat. Cell Biol.* 10:955–63

Arana E, Vehlow A, Harwood NE, Vigorito E, Henderson R, et al. 2008. Activation of the small GTPase Rac2 via the B cell receptor regulates B cell adhesion and immunological-synapse formation. *Immunity* 28:88–99

Arts EGJM, Jager S, Hoekstra D. 1994. Evidence for the existence of lipid-diffusion barriers in the equatorial segment of human spermatozoa. *Biochem. J.* 304:211–18

Axelrod D, Ravdin P, Koppel DE, Schlessinger J, Webb WW, et al. 1976. Lateral motion of fluorescently labeled acetylcholine receptors in membranes of developing muscle-fibers. *Proc. Natl. Acad. Sci. USA* 73:4594–98

Baier CJ, Gallegos CE, Levi V, Barrantes FJ. 2010. Cholesterol modulation of nicotinic acetylcholine receptor surface mobility. *Eur. Biophys. J.* 39:213–27

Bauer M, Pelkmans L. 2006. A new paradigm for membrane-organizing and -shaping scaffolds. *FEBS Lett.* 580:5559–64

Baumgart T, Hammond AT, Sengupta P, Hess ST, Holowka DA, et al. 2007. Large-scale fluid/fluid phase separation of proteins and lipids in giant plasma membrane vesicles. *Proc. Natl. Acad. Sci. USA* 104:3165–70

Baumgartner W, Schutz GJ, Wiegand J, Golenhofen N, Drenckhahn D. 2003. Cadherin function probed by laser tweezer and single molecule fluorescence in vascular endothelial cells. *J. Cell Sci.* 116:1001–11

Benda A, Benes M, Marecek V, Lhotsky A, Hermens WT, Hof M. 2003. How to determine diffusion coefficients in planar phospholipid systems by confocal fluorescence correlation spectroscopy. *Langmuir* 19:4120–26

Boggs JM, Wang HM. 2004. Co-clustering of galactosylceramide and membrane proteins in oligodendrocyte membranes on interaction with polyvalent carbohydrate and prevention by an intact cytoskeleton. *J. Neurosci. Res.* 76:342–55

Boiko T, Vakulenko M, Ewers H, Yap CC, Norden C, Winckler B. 2007. Ankyrin-dependent and -independent mechanisms orchestrate axonal compartmentalization of L1 family members neurofascin and L1/neuron-glia cell adhesion molecule. *J. Neurosci.* 27:590–603

Boucrot E, Saffarian S, Massol R, Kirchhausen T, Ehrlich M. 2006. Role of lipids and actin in the formation of clathrin-coated pits. *Exp. Cell Res.* 312:4036–48

Brachet A, Leterrier C, Irondelle M, Fache MP, Racine V, et al. 2010. Ankyrin G restricts ion channel diffusion at the axonal initial segment before the establishment of the diffusion barrier. *J. Cell Biol.* 191:383–95

Branden C, Tooze J. 1999. *Introduction to Protein Structure*. New York: Garland. 2nd ed.

Bretscher A. 1999. Regulation of cortical structure by the ezrin-radixin-moesin protein family. *Curr. Opin. Cell. Biol.* 11:109–16

Briegel A, Ortega DR, Tocheva EI, Wuichet K, Li Z, et al. 2009. Universal architecture of bacterial chemoreceptor arrays. *Proc. Natl. Acad. Sci. USA* 106:17181–86

Bruckbauer A, Dunne PD, James P, Howes E, Zhou DJ, et al. 2010. Selective diffusion barriers separate membrane compartments. *Biophys. J.* 99:L1–L3

Bussell SJ, Hammer DA, Koch DL. 1994. The effect of hydrodynamic interactions on the tracer and gradient diffusion of integral membrane proteins in lipid bilayers. *J. Fluid Mech.* 258:167–90

Bussell SJ, Koch DL, Hammer DA. 1995a. Effect of hydrodynamic interactions on the diffusion of integral membrane proteins: tracer diffusion in organelle and reconstituted membranes. *Biophys. J.* 68:1828–35

Bussell SJ, Koch DL, Hammer DA. 1995b. Effect of hydrodynamic interactions on the diffusion of integral membrane proteins: diffusion in plasma membranes. *Biophys. J.* 68:1836–49

Campelo F, Fabrikant G, McMahon HT, Kozlov MM. 2010. Modeling membrane shaping by proteins: focus on EHD2 and N-BAR domains. *FEBS Lett.* 584:1830–39

Carramusa L, Ballestrem C, Zilberman Y, Bershadsky AD. 2007. Mammalian diaphanous-related formin Dia1 controls the organization of E-cadherin-mediated cell-cell junctions. *J. Cell Sci.* 120:3870–82

Caudron F, Barral Y. 2009. Septins and the lateral compartmentalization of eukaryotic membranes. *Dev. Cell* 16:493–506

Cavey M, Lecuit T. 2009. Molecular bases of cell-cell junctions stability and dynamics. *Cold Spring Harb. Perspect. Biol.* 1:a002998

Chang CH, Takeuchi H, Ito T, Machida K, Ohnishi S. 1981. Lateral mobility of erythrocyte membrane proteins studied by the fluorescence photobleaching recovery technique. *J. Biochem.* 90:997–1004
Chaudhuri A, Bhattacharya B, Gowrishankar K, Mayor S, Rao M. 2011. Spatiotemporal regulation of chemical reactions by active cytoskeletal remodeling. *Proc. Natl. Acad. Sci. USA* 108:14825–30
Chen Y, Veracini L, Benistant C, Jacobson K. 2009. The transmembrane protein CBP plays a role in transiently anchoring small clusters of Thy-1, a GPI-anchored protein, to the cytoskeleton. *J. Cell Sci.* 122:3966–72
Chien MP, Lin CH, Chang DK. 2009. Recruitment of HIV-1 envelope occurs subsequent to lipid mixing: a fluorescence microscopic evidence. *Retrovirology* 6:20
Chung I, Akita R, Vandlen R, Toomre D, Schlessinger J, Mellman I. 2010. Spatial control of EGF receptor activation by reversible dimerization on living cells. *Nature* 464:783–87
Ciobanasu C, Siebrasse JP, Kubitscheck U. 2010. Cell-penetrating HIV1 TAT peptides can generate pores in model membranes. *Biophys. J.* 99:153–62
Co C, Wong DT, Gierke S, Chang V, Taunton J. 2007. Mechanism of actin network attachment to moving membranes: barbed-end capture by N-WASP WH2 domains. *Cell* 128:901–13
Cowan AE, Myles DG, Koppel DE. 1987. Lateral diffusion of the PH-20 protein on guinea pig sperm: evidence that barriers to diffusion maintain plasma membrane domains in mammalian sperm. *J. Cell Biol.* 104:917–23
Crane JM, Verkman AS. 2008. Long-range nonanomalous diffusion of quantum dot-labeled aquaporin-1 water channels in the cell plasma membrane. *Biophys. J.* 94:702–13
de Monvel JB, Brownell WE, Ulfendahl M. 2006. Lateral diffusion anisotropy and membrane lipid/skeleton interaction in outer hair cells. *Biophys. J.* 91:364–81
Dietrich C, Volovyk ZN, Levi M, Thompson NL, Jacobson K. 2001. Partitioning of Thy-1, GM1, and cross-linked phospholipid analogs into lipid rafts reconstituted in supported model membrane monolayers. *Proc. Natl. Acad. Sci. USA* 98:10642–47
Dodd TL, Hammer DA, Sangani AS, Koch DL. 1995. Numerical simulations of the effect of hydrodynamic interactions on diffusivities of integral membrane proteins. *J. Fluid Mech.* 293:147–80
Doherty GJ, McMahon HT. 2008. Mediation, modulation, and consequences of membrane-cytoskeleton interactions. *Annu. Rev. Biophys.* 37:65–95
Douglass AD, Vale RD. 2005. Single-molecule microscopy reveals plasma membrane microdomains created by protein-protein networks that exclude or trap signaling molecules in T cells. *Cell* 121:937–50
Dustin ML, Depoil D. 2011. New insights into the T cell synapse from single molecule techniques. *Nat. Rev. Immunol.* 11:672–84
Eggeling C, Ringemann C, Medda R, Schwarzmann G, Sandhoff K, et al. 2009. Direct observation of the nanoscale dynamics of membrane lipids in a living cell. *Nature* 457:1159–62
Ehrig J, Petrov EP, Schwille P. 2011. Near-critical fluctuations and cytoskeleton-assisted phase separation lead to subdiffusion in cell membranes. *Biophys. J.* 100:80–89
Ehrlich M, Boll W, van Oijen A, Hariharan R, Chandran K, et al. 2004. Endocytosis by random initiation and stabilization of clathrin-coated pits. *Cell* 118:591–605
Engelman DM. 2005. Membranes are more mosaic than fluid. *Nature* 438:578–80
Evans E, Ritchie K. 1999. Strength of a weak bond connecting flexible polymer chains. *Biophys. J.* 76:2439–47
Febo-Ayala W, Morera-Felix SL, Hrycyna CA, Thompson DH. 2006. Functional reconstitution of the integral membrane enzyme, isoprenylcysteine carboxyl methyltransferase, in synthetic bolalipid membrane vesicles. *Biochemistry* 45:14683–94
Field KA, Holowka D, Baird B. 1997. Compartmentalized activation of the high affinity immunoglobulin E receptor within membrane domains. *J. Biol. Chem.* 272:4276–80
Fleire SJ, Goldman JP, Carrasco YR, Weber M, Bray D, Batista FD. 2006. B cell ligand discrimination through a spreading and contraction response. *Science* 312:738–41
Francis SS, Sfakianos J, Lo B, Mellman I. 2011. A hierarchy of signals regulates entry of membrane proteins into the ciliary membrane domain in epithelial cells. *J. Cell Biol.* 193:219–33
Frick M, Schmidt K, Nichols BJ. 2007. Modulation of lateral diffusion in the plasma membrane by protein density. *Curr. Biol.* 17:462–67
Fu G, Wang C, Liu L, Wang GY, Chen YZ, Xu ZZ. 2008. Heterodimerization of integrin Mac-1 subunits studied by single-molecule imaging. *Biochem. Biophys. Res. Commun.* 368:882–86

Fujiwara T, Ritchie K, Murakoshi H, Jacobson K, Kusumi A. 2002. Phospholipids undergo hop diffusion in compartmentalized cell membrane. *J. Cell Biol.* 157:1071–81
Gambin Y, Lopez-Esparza R, Reffay M, Sierecki E, Gov NS, et al. 2006. Lateral mobility of proteins in liquid membranes revisited. *Proc. Natl. Acad. Sci. USA* 103:2098–102
Garg S, Tang JX, Ruhe J, Naumann CA. 2009. Actin-induced perturbation of PS lipid-cholesterol interaction: a possible mechanism of cytoskeleton-based regulation of membrane organization. *J. Struct. Biol.* 168:11–20
Gaus K, Le Lay S, Balasubramanian N, Schwartz MA. 2006. Integrin-mediated adhesion regulates membrane order. *J. Cell Biol.* 174:725–34
Gowrishankar K, Ghosh S, Saha SCR, Mayor S, Rao M. 2012. Active remodeling of cortical actin regulates spatiotemporal organization of cell surface molecules. *Cell* 149:1353–67
Golan DE, Brown CS, Cianci CML, Furlong ST, Caulfield JP. 1986. Schistosomula of *Schistosoma mansoni* use lysophosphatidylcholine to lyse adherent human red blood cells and immobilize red cell membrane components. *J. Cell Biol.* 103:819–28
Golan DE, Veatch W. 1980. Lateral mobility of band 3 in the human erythrocyte membrane studied by fluorescence photobleaching recovery: evidence for control by cytoskeletal interactions. *Proc. Natl. Acad. Sci. USA* 77:2537–41
Gomez-Mouton C, Abad JL, Mira E, Lacalle RA, Gallardo E, et al. 2001. Segregation of leading edge and uropod components into specific lipid rafts during T cell polarization. *Proc. Natl. Acad. Sci. USA* 98:9642–47
Goswami D, Gowrishankar K, Bilgrami S, Ghosh S, Raghupathy R, et al. 2008. Nanoclusters of GPI-anchored proteins are formed by cortical actin-driven activity. *Cell* 135:1085–97
Grecco HE, Schmick M, Bastiaens PI. 2011. Signaling from the living plasma membrane. *Cell* 144:897–909
Groves JT, Kuriyan J. 2010. Molecular mechanisms in signal transduction at the membrane. *Nat. Struct. Mol. Biol.* 17:659–65
Haggie PM, Kim JK, Lukacs GL, Verkman AS. 2006. Tracking of quantum dot-labeled CFTR shows near immobilization by C-terminal PDZ interactions. *Mol. Biol. Cell* 17:4937–45
Harding AS, Hancock JF. 2008. Using plasma membrane nanoclusters to build better signaling circuits. *Trends Cell Biol.* 18:364–71
Hartman NC, Groves JT. 2011. Signaling clusters in the cell membrane. *Curr. Opin. Cell Biol.* 23:370–76
Hashimoto-Tane A, Yokosuka T, Sakata-Sogawa K, Sakuma M, Ishihara C, et al. 2011. Dynein-driven transport of T cell receptor microclusters regulates immune synapse formation and T cell activation. *Immunity* 34:919–31
Heinrich R, Neel BG, Rapoport TA. 2002. Mathematical models of protein kinase signal transduction. *Mol. Cell* 9:957–70
Hess ST, Gould TJ, Gudheti MV, Maas SA, Mills KD, Zimmerberg J. 2007. Dynamic clustered distribution of hemagglutinin resolved at 40 nm in living cell membranes discriminates between raft theories. *Proc. Natl. Acad. Sci. USA* 104:17370–75
Honerkamp-Smith AR, Cicuta P, Collins MD, Veatch SL, den Nijs M, et al. 2008. Line tensions, correlation lengths, and critical exponents in lipid membranes near critical points. *Biophys. J.* 95:236–46
Hu QC, Milenkovic L, Jin H, Scott MP, Nachury MV, et al. 2010. A septin diffusion barrier at the base of the primary cilium maintains ciliary membrane protein distribution. *Science* 329:436–39
Huang J, Zarnitsyna VI, Liu BY, Edwards LJ, Jiang N, et al. 2010. The kinetics of two-dimensional TCR and pMHC interactions determine T-cell responsiveness. *Nature* 464:932–36
Huppa JB, Axmann M, Mortelmaier MA, Lillemeier BF, Newell EW, et al. 2010. TCR-peptide-MHC interactions in situ show accelerated kinetics and increased affinity. *Nature* 463:963–67
Ichikawa T, Aoki T, Takeuchi Y, Yanagida T, Ide T. 2006. Immobilizing single lipid and channel molecules in artificial lipid bilayers with annexin A5. *Langmuir* 22:6302–7
Ihara M, Kinoshita A, Yamada S, Tanaka H, Tanigaki A, et al. 2005. Cortical organization by the septin cytoskeleton is essential for structural and mechanical integrity of mammalian spermatozoa. *Dev. Cell* 8:343–52
Iino R, Koyama I, Kusumi A. 2001. Single molecule imaging of green fluorescent proteins in living cells: E-cadherin forms oligomers on the free cell surface. *Biophys. J.* 80:2667–77

Imjeti NS, Lebreton S, Paladino S, de la Fuente E, Gonzales A, Zurzolo C. 2011. N-glycosylation instead of cholesterol mediates oligomerization and apical sorting of GPI-APs in FRT cells. *Mol. Biol. Cell* 22:4621–34

Jaqaman K, Kuwata H, Touret N, Collins R, Trimble WS, et al. 2011. Cytoskeletal control of CD36 diffusion promotes its receptor and signaling function. *Cell* 146:593–606

Kahya N, Pecheur EI, de Boeij WP, Wiersma DA, Hoekstra D. 2001. Reconstitution of membrane proteins into giant unilamellar vesicles via peptide-induced fusion. *Biophys. J.* 81:1464–74

Kaiser HJ, Lingwood D, Levental I, Sampaio JL, Kalvodova L, et al. 2009. Order of lipid phases in model and plasma membranes. *Proc. Natl. Acad. Sci. USA* 106:16645–50

Kaizuka Y, Douglass AD, Vardhana S, Dustin ML, Vale RD. 2009. The coreceptor CD2 uses plasma membrane microdomains to transduce signals in T cells. *J. Cell Biol.* 185:521–34

Kalay Z, Fujiwara TK, Kusumi A. 2012. Confining domains lead to reaction bursts: reaction kinetics in the plasma membrane. *PLoS One* 7:e32948

Kalay Z, Parris PE, Kenkre VM. 2008. Effects of disorder in location and size of fence barriers on molecular motion in cell membranes. *J. Phys. Condens. Matter* 20:245105

Kapitza HG, Ruppel DA, Galla HJ, Sackmann E. 1984. Lateral diffusion of lipids and glycophorin in solid phosphatidylcholine bilayers. The role of structural defects. *Biophys. J.* 45:577–87

Katsuki T, Joshi R, Ailani D, Hiromi Y. 2011. Compartmentalization within neurites: its mechanisms and implications. *Dev. Neurobiol.* 71:458–73

Kenkre VM, Giuggioli L, Kalay Z. 2008. Molecular motion in cell membranes: analytic study of fence-hindered random walks. *Phys. Rev. E* 77:051907

Kenworthy AK, Nichols BJ, Remmert CL, Hendrix GM, Kumar M, et al. 2004. Dynamics of putative raft-associated proteins at the cell surface. *J. Cell Biol.* 165:735–46

Kholodenko BN, Hancock JF, Kolch W. 2010. Signalling ballet in space and time. *Nat. Rev. Mol. Cell Biol.* 11:414–26

Kirchhausen T. 2009. Imaging endocytic clathrin structures in living cells. *Trends Cell Biol.* 19:596–605

Klarlund JK. 1985. Transformation of cells by an inhibitor of phosphatases acting on phosphotyrosine in proteins. *Cell* 41:707–17

Kobayashi T, Storrie B, Simons K, Dotti CG. 1992. A functional barrier to movement of lipids in polarized neurons. *Nature* 359:647–50

Kodippili GC, Spector J, Sullivan C, Kuypers FA, Labotka R, et al. 2009. Imaging of the diffusion of single band 3 molecules on normal and mutant erythrocytes. *Blood* 113:6237–45

Kusumi A, Fujiwara TK, Morone N, Yoshida KJ, Chadda R, et al. 2012. Membrane mechanisms for signal transduction: the coupling of the meso-scale raft domains to membrane-skeleton-induced compartments and dynamic protein complexes. *Semin. Cell Dev. Biol.* 23:126–44

Kusumi A, Koyama-Honda I, Suzuki K. 2004. Molecular dynamics and interactions for creation of stimulation-induced stabilized rafts from small unstable steady-state rafts. *Traffic* 5:213–30

Kusumi A, Nakada C, Ritchie K, Murase K, Suzuki K, et al. 2005. Paradigm shift of the plasma membrane concept from the two-dimensional continuum fluid to the partitioned fluid: high-speed single-molecule tracking of membrane molecules. *Annu. Rev. Biophys. Biomol. Struct.* 34:351–U54

Kusumi A, Sako Y. 1996. Cell surface organization by the membrane skeleton. *Curr. Opin. Cell Biol.* 8:566–74

Kusumi A, Shirai YM, Koyama-Honda I, Suzuki KGN, Fujiwara TK. 2010. Hierarchical organization of the plasma membrane: investigations by single-molecule tracking versus fluorescence correlation spectroscopy. *FEBS Lett.* 584:1814–23

Kusumi A, Suzuki KG, Kasai RS, Ritchie K, Fujiwara TK. 2011. Hierarchical mesoscale domain organization of the plasma membrane. *Trends Biochem. Sci.* 36:604–15

Kusumi A, Sako Y, Yamamoto M. 1993. Confined lateral diffusion of membrane receptors as studied by single particle tracking (nanovid microscopy). Effects of calcium-induced differentiation in cultured epithelial cells. *Biophys J.* 65:2021–40

Kwitny S, Klaus AV, Hunnicutt GR. 2010. The annulus of the mouse sperm tail is required to establish a membrane diffusion barrier that is engaged during the late steps of spermiogenesis. *Biol. Reprod.* 82:669–78

Ladha S, Mackie AR, Harvey LJ, Clark DC, Lea EJA, et al. 1996. Lateral diffusion in planar lipid bilayers: a fluorescence recovery after photobleaching investigation of its modulation by lipid composition, cholesterol, or alamethicin content and divalent cations. *Biophys. J.* 71:1364–73

Lajoie P, Goetz JG, Dennis JW, Nabi IR. 2009. Lattices, rafts, and scaffolds: domain regulation of receptor signaling at the plasma membrane. *J. Cell Biol.* 185:381–85

Lajoie P, Partridge EA, Guay G, Goetz JG, Pawling J, et al. 2007. Plasma membrane domain organization regulates EGFR signaling in tumor cells. *J. Cell Biol.* 179:341–56

Larson DR, Gosse JA, Holowka DA, Baird BA, Webb WW. 2005. Temporally resolved interactions between antigen-stimulated IgE receptors and Lyn kinase on living cells. *J. Cell Biol.* 171:527–36

Lasserre R, Guo XJ, Conchonaud F, Hamon Y, Hawchar O, et al. 2008. Raft nanodomains contribute to Akt/PKB plasma membrane recruitment and activation. *Nat. Chem. Biol.* 4:538–47

Lauffenburger D, Linderman J. 1993. *Receptors*. New York: Oxford Univ. Press

Lee GM, Zhang F, Ishihara A, McNeil CL, Jacobson KA. 1993. Unconfined lateral diffusion and an estimate of pericellular matrix viscosity revealed by measuring the mobility of gold-tagged lipids. *J. Cell Biol.* 120:25–35

Lenne PF, Wawrezinieck L, Conchonaud F, Wurtz O, Boned A, et al. 2006. Dynamic molecular confinement in the plasma membrane by microdomains and the cytoskeleton meshwork. *EMBO J.* 25:3245–56

Lerea KM, Tonks NK, Krebs EG, Fischer EH, Glomset JA. 1989. Vanadate and molybdate increase tyrosine phosphorylation in a 50-kilodalton protein and stimulate secretion in electropermeabilized platelets. *Biochemistry* 28:9286–92

Levental I, Grzybek M, Simons K. 2011. Raft domains of variable properties and compositions in plasma membrane vesicles. *Proc. Natl. Acad. Sci. USA* 108:11411–16

Levental I, Lingwood D, Grzybek M, Coskun U, Simons K. 2010. Palmitoylation regulates raft affinity for the majority of integral raft proteins. *Proc. Natl. Acad. Sci. USA* 107:22050–54

Lin KBL, Freeman SA, Zabetian S, Brugger H, Weber M, et al. 2008. The Rap GTPases regulate B cell morphology, immune-synapse formation, and signaling by particulate B cell receptor ligands. *Immunity* 28:75–87

Lindblom G, Johansson LBA, Arvidson G. 1981. Effect of cholesterol in membranes. Pulsed nuclear-magnetic-resonance measurements of lipid lateral diffusion. *Biochemistry* 20:2204–7

Lingwood D, Ries J, Schwille P, Simons K. 2008. Plasma membranes are poised for activation of raft phase coalescence at physiological temperature. *Proc. Natl. Acad. Sci. USA* 105:10005–10

Lingwood D, Simons K. 2010. Lipid rafts as a membrane-organizing principle. *Science* 327:46–50

Liu CH, Paprica A, Petersen NO. 1997. Effects of size of macrocyclic polyamides on their rate of diffusion in model membranes. *Biophys. J.* 73:2580–87

Liu WL, Meckel T, Tolar P, Sohn HW, Pierce SK. 2010. Intrinsic properties of immunoglobulin IgG1 isotype-switched B cell receptors promote microclustering and the initiation of signaling. *Immunity* 32:778–89

Lommerse PHM, Snaar-Jagaiska BE, Spaink HP, Schmidt T. 2005. Single-molecule diffusion measurements of H-Ras at the plasma membrane of live cells reveal microdomain localization upon activation. *J. Cell Sci.* 118:1799–809

Lommerse PH, Vastenhoud K, Pirinen NJ, Magee AI, Spaink HP, Schmidt T. 2006. Single-molecule diffusion reveals similar mobility for the Lck, H-ras, and K-ras membrane anchors. *Biophys J.* 91:1090–97

Manzo C, van Zanten TS, Garcia-Parajo MF. 2011. Nanoscale fluorescence correlation spectroscopy on intact living cell membranes with NSOM probes. *Biophys. J.* 100:L8–10

McMahon HT, Boucrot E. 2011. Molecular mechanism and physiological functions of clathrin-mediated endocytosis. *Nat. Rev. Mol. Cell Biol.* 12:517–33

Mercer J, Schelhaas M, Helenius A. 2010. Virus entry by endocytosis. *Annu. Rev. Biochem.* 79:803–33

Merkel R, Nassoy P, Leung A, Ritchie K, Evans E. 1999. Energy landscapes of receptor-ligand bonds explored with dynamic force spectroscopy. *Nature* 397:50–53

Miettinen HM, Matter K, Hunziker W, Rose JK, Mellman I. 1992. Fc receptor endocytosis is controlled by a cytoplasmic domain determinant that actively prevents coated pit localization. *J. Cell Biol.* 116:875–88

Miettinen HM, Rose JK, Mellman I. 1989. Fc receptor isoforms exhibit distinct abilities for coated pit localization as a result of cytoplasmic domain heterogeneity. *Cell* 58:317–27

Minguet S, Swamy M, Alarcon B, Luescher IF, Schamel WWA. 2007. Full activation of the T cell receptor requires both clustering and conformational changes at CD3. *Immunity* 26:43–54

Mocciaro A, Schiebel E. 2010. Cdc14: a highly conserved family of phosphatases with non-conserved functions? *J. Cell Sci.* 123:2867–76

Moerner WE. 2002. Single-molecule optical spectroscopy of autofluorescent proteins. *J. Chem. Phys.* 117:10925–37

Morone N, Fujiwara T, Murase K, Kasai RS, Ike H, et al. 2006. Three-dimensional reconstruction of the membrane skeleton at the plasma membrane interface by electron tomography. *J. Cell Biol.* 174:851–62

Mossman KD, Campi G, Groves JT, Dustin ML. 2005. Altered TCR signaling from geometrically repatterned immunological synapses. *Science* 310:1191–93

Mueller V, Ringemann C, Honigmann A, Schwarzmann G, Medda R, et al. 2011. STED nanoscopy reveals molecular details of cholesterol- and cytoskeleton-modulated lipid interactions in living cells. *Biophys. J.* 101:1651–60

Murakoshi H, Iino R, Kobayashi T, Fujiwara T, Ohshima C, et al. 2004. Single-molecule imaging analysis of Ras activation in living cells. *Proc. Natl. Acad. Sci. USA* 101:7317–22

Murase K, Fujiwara T, Umemura Y, Suzuki K, Iino R, et al. 2004. Ultrafine membrane compartments for molecular diffusion as revealed by single molecule techniques. *Biophys. J.* 86:4075–93

Murcia MJ, Minner DE, Mustata GM, Ritchie K, Naumann CA. 2008. Design of quantum dot-conjugated lipids for long-term, high-speed tracking experiments on cell surfaces. *J. Am. Chem. Soc.* 130:15054–62

Nabi IR, ed. 2011. *Cellular Domains*. Hoboken, NJ: Wiley-Blackwell

Nachury MV, Seeley ES, Jin H. 2010. Trafficking to the ciliary membrane: how to get across the periciliary diffusion barrier? *Annu. Rev. Cell Dev. Biol.* 26:59–87

Nakada C, Ritchie K, Oba Y, Nakamura M, Hotta Y, et al. 2003. Accumulation of anchored proteins forms membrane diffusion barriers during neuronal polarization. *Nat. Cell Biol.* 5:626–32

Nicolau DV, Burrage K, Parton RG, Hancock JF. 2006. Identifying optimal lipid raft characteristics required to promote nanoscale protein-protein interactions on the plasma membrane. *Mol. Cell. Biol.* 26:313–23

Nicolau DV, Hancock JF, Burrage K. 2007. Sources of anomalous diffusion on cell membranes: a Monte Carlo study. *Biophys. J.* 92:1975–87

Niehaus AM, Vlachos DG, Edwards JS, Plechac P, Tribe R. 2008. Microscopic simulation of membrane molecule diffusion on corralled membrane surfaces. *Biophys. J.* 94:1551–64

Nikolaev VO, Moshkov A, Lyon AR, Miragoli M, Novak P, et al. 2010. β2-adrenergic receptor redistribution in heart failure changes cAMP compartmentation. *Science* 327:1653–57

Nishimura SY, Vrljic M, Klein LO, McConnell HM, Moerner WE. 2006. Cholesterol depletion induces solid-like regions in the plasma membrane. *Biophys. J.* 90:927–38

Novikov DS, Fieremans E, Jensen JH, Helpern JA. 2011. Random walk with barriers. *Nat. Phys.* 7:508–14

O'Connell KMS, Rolig AS, Whitesell JD, Tamkun MM. 2006. Kv2.1 potassium channels are retained within dynamic cell surface microdomains that are defined by a perimeter fence. *J. Neurosci.* 26:9609–18

Paladino S, Lebreton S, Tivodar S, Campana V, Tempre R, Zurzolo C. 2008. Different GPI-attachment signals affect the oligomerisation of GPI-anchored proteins and their apical sorting. *J. Cell Sci.* 121:4001–7

Parton RG, Hancock JF. 2004. Lipid rafts and plasma membrane microorganization: insights from Ras. *Trends Cell Biol.* 14:141–47

Parton RG, Hanzal-Bayer M, Hancock JF. 2006. Biogenesis of caveolae: a structural model for caveolin-induced domain formation. *J. Cell Sci.* 119:787–96

Parton RG, Simons K. 2007. The multiple faces of caveolae. *Nat. Rev. Mol. Cell Biol.* 8:185–94

Pasenkiewicz-Gierula M, Subczynski WK, Kusumi A. 1991. Influence of phospholipid unsaturation on the cholesterol distribution in membranes. *Biochimie* 73:1311–16

Peters R, Cherry RJ. 1982. Lateral and rotational diffusion of bacteriorhodopsin in lipid bilayers: experimental test of the Saffman-Delbruck equations. *Proc. Natl. Acad. Sci. USA* 79:4317–21

Petrini EM, Marchionni I, Zacchi P, Sieghart W, Cherubini E. 2004. Clustering of extrasynaptic $GABA_A$ receptors modulates tonic inhibition in cultured hippocampal neurons. *J. Biol. Chem.* 279:45833–43

Pierce SK, Liu WL. 2010. The tipping points in the initiation of B cell signalling: how small changes make big differences. *Nat. Rev. Immunol.* 10:767–77

Platta HW, Stenmark H. 2011. Endocytosis and signaling. *Curr. Opin. Cell Biol.* 23:393–403
Powles JG, Mallett MJD, Rickayzen G, Evans WAB. 1992. Exact analytic solutions for diffusion impeded by an infinite array of partially permeable barriers. *Proc. R. Soc. Lond. Ser. A* 436:391–403
Pralle A, Keller P, Florin EL, Simons K, Horber JKH. 2000. Sphingolipid-cholesterol rafts diffuse as small entities in the plasma membrane of mammalian cells. *J. Cell Biol.* 148:997–1007
Prior IA, Hancock JF. 2011. Ras trafficking, localization and compartmentalized signalling. *Semin. Cell Dev. Biol.* Epub ahead of print
Ratto TV, Longo ML. 2002. Obstructed diffusion in phase-separated lipid bilayers: a combined atomic force microscopy and fluorescence recovery after photobleaching approach. *Biophys. J.* 83:3380–92
Roccamo AM, Pediconi MF, Aztiria E, Zanello L, Wolstenholme A, Barrantes FJ. 1999. Cells defective in sphingolipids biosynthesis express low amounts of muscle nicotinic acetylcholine receptor. *Eur. J. Neurosci.* 11:1615–23
Rodgers W, Zavzavadjian J. 2001. Glycolipid-enriched membrane domains are assembled into membrane patches by associating with the actin cytoskeleton. *Exp. Cell Res.* 267:173–83
Rothberg KG, Heuser JE, Donzell WC, Ying YS, Glenney JR, Anderson RG. 1992. Caveolin, a protein component of caveolae membrane coats. *Cell* 68:673–82
Saffman PG, Delbruck M. 1975. Brownian motion in biological membranes. *Proc. Natl. Acad. Sci. USA* 72:3111–13
Sahl SJ, Leutenegger M, Hilbert M, Hell SW, Eggeling C. 2010. Fast molecular tracking maps nanoscale dynamics of plasma membrane lipids. *Proc. Natl. Acad. Sci. USA* 107:6829–34
Sako Y, Kusumi A. 1994. Compartmentalized structure of the plasma-membrane for receptor movements as revealed by a nanometer-level motion analysis. *J. Cell Biol.* 125:1251–64
Sako Y, Nagafuchi A, Tsukita S, Takeichi M, Kusumi A. 1998. Cytoplasmic regulation of the movement of E-cadherin on the free cell surface as studied by optical tweezers and single particle tracking: corralling and tethering by the membrane skeleton. *J. Cell Biol.* 140:1227–40
Samiee KT, Moran-Mirabal JM, Cheung YK, Craighead HG. 2006. Zero mode waveguides for single-molecule spectroscopy on lipid membranes. *Biophys. J.* 90:3288–99
Saxton MJ. 1987. Lateral diffusion in an archipelago. The effect of mobile obstacles. *Biophys. J.* 52:989–97
Saxton MJ. 1990. Lateral diffusion in a mixture of mobile and immobile particles. A Monte-Carlo study. *Biophys. J.* 58:1303–6
Saxton MJ. 2002. Chemically limited reactions on a percolation cluster. *J. Chem. Phys.* 116:203–8
Saxton MJ. 2007. A biological interpretation of transient anomalous subdiffusion. I. Qualitative model. *Biophys. J.* 92:1178–91
Saxton MJ, Jacobson K. 1997. Single-particle tracking: applications to membrane dynamics. *Annu. Rev. Biophys. Biomol. Struct.* 26:373–99
Schaaf MJ, Koopmans WJ, Meckel T, van Noort J, Snaar-Jagalska BE, et al. 2009. Single-molecule microscopy reveals membrane microdomain organization of cells in a living vertebrate. *Biophys. J.* 97:1206–14
Schmidt K, Nichols BJ. 2004. A barrier to lateral diffusion in the cleavage furrow of dividing mammalian cells. *Curr. Biol.* 14:1002–6
Schutz GJ, Kada G, Pastushenko VP, Schindler H. 2000. Properties of lipid microdomains in a muscle cell membrane visualized by single molecule microscopy. *EMBO J.* 19:892–901
Sengupta P, Jovanovic-Talisman T, Skoko D, Renz M, Veatch SL, Lippincott-Schwartz J. 2011. Probing protein heterogeneity in the plasma membrane using PALM and pair correlation analysis. *Nat. Methods* 8:969–75
Sens P, Johannes L, Bassereau P. 2008. Biophysical approaches to protein-induced membrane deformations in trafficking. *Curr. Opin. Cell Biol.* 20:476–82
Sharma P, Varma R, Sarasij RC, Ira, Gousset K, et al. 2004. Nanoscale organization of multiple GPI-anchored proteins in living cell membranes. *Cell* 116:577–89
Sheets ED, Holowka D, Baird B. 1999. Critical role for cholesterol in Lyn-mediated tyrosine phosphorylation of FcεRI and their association with detergent-resistant membranes. *J. Cell Biol.* 145:877–87
Sheetz MP, Schindler M, Koppel DE. 1980. Lateral mobility of integral membrane proteins is increased in spherocytic erythrocytes. *Nature* 285:510–12

Shvartsman DE, Donaldson JC, Diaz B, Gutman O, Martin GS, Henis YI. 2007. Src kinase activity and SH2 domain regulate the dynamics of Src association with lipid and protein targets. *J. Cell Biol.* 178:675–86

Simmonds AC, East JM, Jones OT, Rooney EK, McWhirter J, Lee AG. 1982. Annular and non-annular binding-sites on the (Ca^{2+} + Mg^{2+})–ATPase. *Biochim. Biophys. Acta* 693:398–406

Simons K, Gerl MJ. 2010. Revitalizing membrane rafts: new tools and insights. *Nat. Rev. Mol. Cell Biol.* 11:688–99

Singer SJ, Nicolson GL. 1972. The fluid mosaic model of the structure of cell membranes. *Science* 175:720–31

Smith LM, Rubenstein JLR, Parce JW, McConnell HM. 1980. Lateral diffusion of M-13 coat protein in mixtures of phosphatidylcholine and cholesterol. *Biochemistry* 19:5907–11

Sohn HW, Tolar P, Jin T, Pierce SK. 2006. Fluorescence resonance energy transfer in living cells reveals dynamic membrane changes in the initiation of B cell signaling. *Proc. Natl. Acad. Sci. USA* 103:8143–48

Sohn HW, Tolar P, Pierce SK. 2008. Membrane heterogeneities in the formation of B cell receptor-Lyn kinase microclusters and the immune synapse. *J. Cell Biol.* 182:367–79

Sonnleitner A, Schutz GJ, Schmidt T. 1999. Free Brownian motion of individual lipid molecules in biomembranes. *Biophys. J.* 77:2638–42

Subczynski WK, Antholine WE, Hyde JS, Kusumi A. 1990. Microimmiscibility and 3-dimensional dynamic structures of phosphatidylcholine cholesterol membranes: translational diffusion of a copper complex in the membrane. *Biochemistry* 29:7936–45

Subczynski WK, Hyde JS, Kusumi A. 1991. Effect of alkyl chain unsaturation and cholesterol intercalation on oxygen-transport in membranes: a pulse ESR spin labeling study. *Biochemistry* 30:8578–90

Subczynski WK, Pasenkiewicz-Gierula M, McElhaney RN, Hyde JS, Kusumi A. 2003. Molecular dynamics of 1-palmitoyl-2-oleoylphosphatidylcholine membranes containing transmembrane α-helical peptides with alternating leucine and alanine residues. *Biochemistry* 42:3939–48

Suetsugu S, Toyooka K, Senju Y. 2010. Subcellular membrane curvature mediated by the BAR domain superfamily proteins. *Semin. Cell Dev. Biol.* 21:340–49

Suzuki K, Ritchie K, Kajikawa E, Fujiwara T, Kusumi A. 2005. Rapid hop diffusion of a G-protein-coupled receptor in the plasma membrane as revealed by single-molecule techniques. *Biophys. J.* 88:3659–80

Suzuki KGN, Fujiwara TK, Edidin M, Kusumi A. 2007a. Dynamic recruitment of phospholipase Cγ at transiently immobilized GPI- anchored receptor clusters induces IP3-Ca^{2+} signaling: single-molecule tracking study 2. *J. Cell Biol.* 177:731–42

Suzuki KGN, Fujiwara TK, Sanematsu F, Iino R, Edidin M, Kusumi A. 2007b. GPI-anchored receptor clusters transiently recruit Lyn and Gα for temporary cluster immobilization and Lyn activation: single-molecule tracking study 1. *J. Cell Biol.* 177:717–30

Suzuki KGN, Kasai RS, Hirosawa KM, Nemoto YL, Ishibashi M, et al. 2012. Transient GPI-anchored protein homodimers are units for raft organization and function. *Nat. Chem. Biol.* In press

Swaisgood M, Schindler M. 1989. Lateral diffusion of lectin receptors in fibroblast membranes as a function of cell-shape. *Exp. Cell Res.* 180:515–28

Tada T, Simonetta A, Batterton M, Kinoshita M, Edbauer D, Sheng M. 2007. Role of septin cytoskeleton in spine morphogenesis and dendrite development in neurons. *Curr. Biol.* 17:1752–58

Takeuchi M, Miyamoto H, Sako Y, Komizu H, Kusumi A. 1998. Structure of the erythrocyte membrane skeleton as observed by atomic force microscopy. *Biophys. J.* 74:2171–83

Takimoto B, Nabika H, Murakoshi K. 2009. Single molecular observation of hop diffusion in a lipid bilayer at metallic nanogates. *J. Phys. Chem. C* 113:3127–32

Takizawa PA, DeRisi JL, Wilhelm JE, Vale RD. 2000. Plasma membrane compartmentalization in yeast by messenger RNA transport and a septin diffusion barrier. *Science* 290:341–44

Tavano R, Contento RL, Baranda SJ, Soligo M, Tuosto L, et al. 2006. CD28 interaction with filamin-A controls lipid raft accumulation at the T-cell immunological synapse. *Nat. Cell Biol.* 8:1270–76

Tolar P, Sohn HW, Pierce SK. 2005. The initiation of antigen-induced B cell antigen receptor signaling viewed in living cells by fluorescence resonance energy transfer. *Nat. Immunol.* 6:1168–76

Tomishige M, Sako Y, Kusumi A. 1998. Regulation mechanism of the lateral diffusion of band 3 in erythrocyte membranes by the membrane skeleton. *J. Cell Biol.* 142:989–1000

Toomre D, Bewersdorf J. 2010. A new wave of cellular imaging. *Annu. Rev. Cell Dev. Biol.* 26:285–314

Treanor B, Depoil D, Gonzalez-Granja A, Barral P, Weber M, et al. 2010. The membrane skeleton controls diffusion dynamics and signaling through the B cell receptor. *Immunity* 32:187–99

Tsuji A, Kawasaki K, Ohnishi S, Merkle H, Kusumi A. 1988. Regulation of band-3 mobilities in erythrocyte ghost membranes by protein association and cytoskeletal meshwork. *Biochemistry* 27:7447–52

Tsuji A, Ohnishi S. 1986. Restriction of the lateral motion of band-3 in the erythrocyte-membrane by the cytoskeletal network: dependence on spectrin association state. *Biochemistry* 25:6133–39

Umemura YM, Vrljic M, Nishimura SY, Fujiwara TK, Suzuki KGN, Kusumi A. 2008. Both MHC class II and its GPI-anchored form undergo hop diffusion as observed by single-molecule tracking. *Biophys. J.* 95:435–50

Vaz WLC, Criado M, Madeira VMC, Schoellmann G, Jovin TM. 1982. Size dependence of the translational diffusion of large integral membrane-proteins in liquid-crystalline phase lipid bilayers: a study using fluorescence recovery after photobleaching. *Biochemistry* 21:5608–12

Vaz WLC, Kapitza HG, Stumpel J, Sackmann E, Jovin TM. 1981. Translational mobility of glycophorin in bilayer-membranes of dimyristoylphosphatidylcholine. *Biochemistry* 20:1392–96

Viola A, Contento RL, Molon B. 2010. Signaling amplification at the immunological synapse. *Immunol. Synapse* 340:109–22

Viola A, Gupta N. 2007. Tether and trap: regulation of membrane-raft dynamics by actin-binding proteins. *Nat. Rev. Immunol.* 7:889–96

Viola A, Schroeder S, Sakakibara Y, Lanzavecchia A. 1999. T lymphocyte costimulation mediated by reorganization of membrane microdomains. *Science* 283:680–82

Vrljic M, Nishimura SY, Brasselet S, Moerner WE, McConnell HM. 2002. Translational diffusion of individual class II MHC membrane proteins in cells. *Biophys J.* 83:2681–92

Vrljic M, Nishimura SY, Moerner WE, McConnell HM. 2005. Cholesterol depletion suppresses the translational diffusion of class II major histocompatibility complex proteins in the plasma membrane. *Biophys. J.* 88:334–47

Wang J, Chen H, Brown EJ. 2001. L-plastin peptide activation of $\alpha_v\beta_3$-mediated adhesion requires integrin conformational change and actin filament disassembly. *J. Biol. Chem.* 276:14474–81

Warren GB, Houslay MD, Metcalfe JC, Birdsall NJM. 1975. Cholesterol is excluded from phospholipid annulus surrounding an active calcium-transport protein. *Nature* 255:684–87

Wenger J, Conchonaud F, Dintinger J, Wawrezinieck L, Ebbesen TW, et al. 2007. Diffusion analysis within single nanometric apertures reveals the ultrafine cell membrane organization. *Biophys. J.* 92:913–19

Wieser S, Moertelmaier M, Fuertbauer E, Stockinger H, Schutz GJ. 2007. (Un)confined diffusion of CD59 in the plasma membrane determined by high-resolution single molecule microscopy. *Biophys. J.* 92:3719–28

Wilbur JD, Hwang PK, Brodsky FM. 2005. New faces of the familiar clathrin lattice. *Traffic* 6:346–50

Winckler B, Forscher P, Mellman I. 1999. A diffusion barrier maintains distribution of membrane proteins in polarized neurons. *Nature* 397:698–701

Winckler B, Poo MM. 1996. No diffusion barrier at axon hillock. *Nature* 379:213–13

Wu M, Holowka D, Craighead HG, Baird B. 2004. Visualization of plasma membrane compartmentalization with patterned lipid bilayers. *Proc. Natl. Acad. Sci. USA* 101:13798–803

Xie YL, Vessey JP, Konecna A, Dahm R, Macchi P, Kiebler MA. 2007. The GTP-binding protein Septin 7 is critical for dendrite branching and dendritic-spine morphology. *Curr. Biol.* 17:1746–51

Yokosuka T, Saito T. 2009. Dynamic regulation of T-cell costimulation through TCR-CD28 microclusters. *Immunol. Rev.* 229:27–40

Yokosuka T, Saito T. 2010. The immunological synapse, TCR microclusters, and T cell activation. *Immunol. Synapse* 340:81–107

Zanoni I, Ostuni R, Capuano G, Collini M, Caccia M, et al. 2009. CD14 regulates the dendritic cell life cycle after LPS exposure through NFAT activation. *Nature* 460:264–68

Annual Review of Cell and Developmental Biology

Volume 28, 2012

Contents

Indexes

Errata

An online log of corrections to *Annual Review of Cell and Developmental Biology* articles may be found at http://cellbio.annualreviews.org/errata.shtml